

UNCLASSIFIED

AD NUMBER
AD446446
NEW LIMITATION CHANGE
TO Approved for public release, distribution unlimited
FROM Distribution authorized to U.S. Gov't. agencies and their contractors; Administrative/Operational Use; JUN 1964. Other requests shall be referred to Office of Civil Defense, Washington, DC.
AUTHORITY
OCD ltr, 13 Jun 1966

THIS PAGE IS UNCLASSIFIED

UNCLASSIFIED

AD 4 4 6 4 4 6

DEFENSE DOCUMENTATION CENTER

FOR

SCIENTIFIC AND TECHNICAL INFORMATION

CAMERON STATION, ALEXANDRIA, VIRGINIA



UNCLASSIFIED

NOTICE: When government or other drawings, specifications or other data are used for any purpose other than in connection with a definitely related government procurement operation, the U. S. Government thereby incurs no responsibility, nor any obligation whatsoever; and the fact that the Government may have formulated, furnished, or in any way supplied the said drawings, specifications, or other data is not to be regarded by implication or otherwise as in any manner licensing the holder or any other person or corporation, or conveying any rights or permission to manufacture, use or sell any patented invention that may in any way be related thereto.

TECHNICAL OPERATIONS RESEARCH

CATALOGED BY D
AS AD No.

446446

THE DOSE RESULTING FROM 1.25 MeV PLANE SOURCE BEHIND
VARIOUS ARRANGEMENTS OF IRON BARRIERS

(Final Report)

By
Dominic J. Raso and Stanley Woolf

Report No. TO-B 64-49
Contract No. OCD-OS-62-219

June, 1964

Submitted to
Office of Civil Defense
Department of Defense
Washington, D. C.

tech ops

DDC AVAILABILITY

Qualified requestors may obtain copies of this report from
the Defense Documentation Center, Alexandria, Virginia 32314.

TECHNICAL OPERATIONS RESEARCH

Subtask 1112B

SUMMARY OF FINAL REPORT

THE DOSE RESULTING FROM 1.25 MeV PLANE SOURCE
BEHIND VARIOUS ARRANGEMENTS OF IRON BARRIERS

(TO-B 64-49)

June, 1964

This is a summary of a report which has been reviewed in the Office of Civil Defense and approved for publication. Approval does not signify that the contents necessarily reflect the views and policies of the Office of Civil Defense.

Contract No. OCD-OS-62-219

Summary Prepared
by Dominic J. Raso
Tech/Ops Research
June, 1964

Burlington, Massachusetts

SUMMARY

A Monte Carlo calculational program is presented that extends the slab geometry programs performed by Technical Operations Research¹⁻⁴ to compute the dose due to scattered photons at various positions for the following geometries:

1. A barrier of various length-to-width ratios and thicknesses
2. Two parallel barriers separated by various distances
(detector located between the barriers)
3. A blockhouse.

Table 1 and Figure 1 show some of the results obtained with a 1.25 MeV plane isotropic source incident on iron. The results in the table and figure are for 5000 photon histories, normalized to one incident photon/cm².

Table 1 contains the scattered dose transmitted through a barrier of 40.5 lbs/ft² of iron. The scattered dose is given for a disk barrier and for rectangular barriers of various length-to-width ratios (1.0, 1.5, 2.0, and 3.0) as a function of solid angle fraction (solid angle divided by 2π) subtended at the detector. It is evident that the scattered dose is almost independent of barrier shape.

Figure 1 shows a comparison of the roof reduction factors computed by Spencer⁵ (the ratio of the detector response in a protected position to the detector response 3 ft above an infinite plane uniformly contaminated) for Co-60 on disk barriers of 20.5, 41.0, and 61.5 lbs/ft² thickness. The abscissa is in units of solid angle fraction, $\omega = 1 - \cos \Theta$. The two methods are in good agreement.

REFERENCES

1. M. J. Berger and D. J. Raso, "Monte Carlo Calculations of Gamma-Ray Backscattering," *Radiation Research* 12, 20-37 (1960).
2. D. J. Raso, "Transmission of Scattered Gamma Rays Through Concrete and Iron Slabs," *Health Physics* 5, 126-141 (1961).
3. D. J. Raso, "Scattering of X-Rays in Laminar Media," *Radiation Research* 19, 384-391 (1963).

4. D. J. Raso, "Monte Carlo Calculations on the Reflection and Transmission of Scattered Gamma Radiations," J. Nuclear Science and Engineering 17, 411-418 (1963).
5. L. V. Spencer, "Structure Shielding Against Fallout Radiation from Nuclear Weapons," National Bureau of Standards Monograph 42 (1962).

TABLE 1
DOSE DUE TO SCATTERING OF PHOTONS THROUGH IRON DISK AND
FOUR IRON SLABS OF VARIOUS LENGTH-TO-WIDTH RATIOS
OF MASS THICKNESS 41.0 psf*

(KeV/g normalized to 1 photon/cm²)

ω	Disk	L = W	L = 1.5 W	L = 2.0 W	L = 3.0 W
† Isotropic					
0.02	0.202	0.203	0.208	0.214	0.200
0.04	0.391	0.417	0.402	0.378	0.390
0.08	0.783	0.790	0.728	0.713	0.700
0.10	0.974	0.966	0.913	0.899	0.853
0.20	1.89	1.92	1.70	1.62	1.56
0.30	2.82	2.75	2.56	2.44	2.30
0.50	4.59	4.53	4.18	4.07	3.95
0.70	6.23	6.19	6.03	5.93	5.79
0.90	7.33	7.29	7.24	7.22	7.30
1.00	7.54	7.54	7.54	7.54	7.54

* 5000 photons of energy 1.25 MeV are assumed incident on the barriers with angles for each of the five cases given by $\cos \Theta_0 = 1.0, 0.75, 0.50, 0.25$, and 0.00 .

† Results for isotropic incidence are obtained by integration of the monodirectional data.

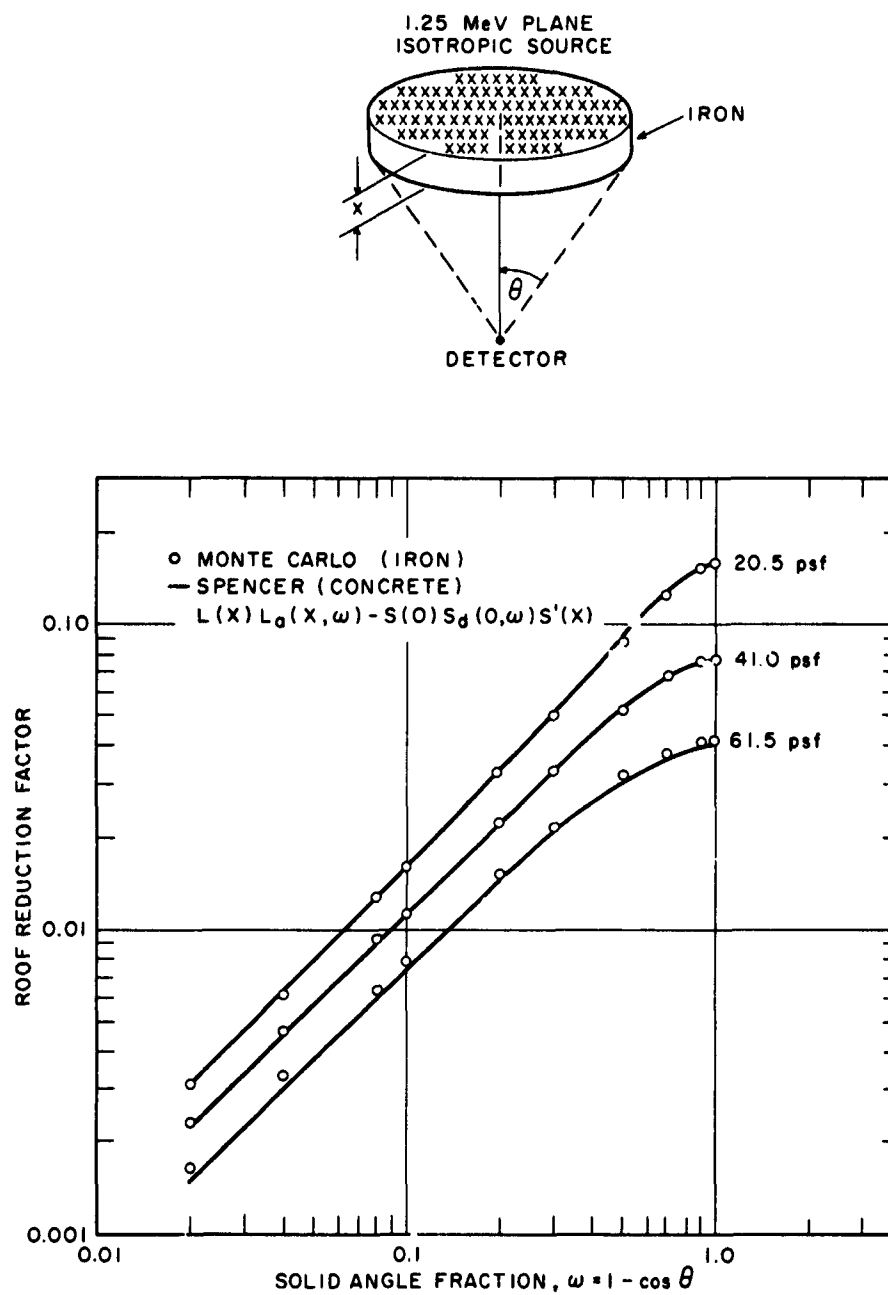


Figure 1. Comparison of Roof Reduction Factors Calculated by the Monte Carlo Method for Iron with that Calculated by the Moment Method for Concrete

THE DOSE RESULTING FROM 1.25 MeV PLANE SOURCE BEHIND
VARIOUS ARRANGEMENTS OF IRON BARRIERS

(Final Report)

By

Dominic J. Raso and Stanley Woolf

Report No. TO-B 64-49

June, 1964

OCD REVIEW NOTICE

This report has been reviewed in the Office of Civil Defense and approved for publication. Approval does not signify that the contents necessarily reflect the views and policies of the Office of Civil Defense.

Prepared for

Office of Civil Defense
Department of Army-OSA
Under
Contract No. OCD-OS-62-219
Subtask 1112B

Burlington, Massachusetts

ABSTRACT

Calculations were performed by the Monte Carlo method to determine the dose at various positions behind parallel barriers (circular or rectangular). Also, calculations were made for a blockhouse geometry. The results were obtained for a 1.25 MeV plane monodirectional source (angles of incidence given by $\cos \Theta_0 = 0.0, 0.25, 0.50, 0.75, 1.0$, and isotropic) incident on 20.5, 41.0, and 61.5 psf of iron. Comparisons were made with roof reduction factors obtained by Spencer and with experiments performed at Technical Operations Research.

TABLE OF CONTENTS

	<u>Page</u>
INTRODUCTION	i
SCHEMATIZATION	1
Case I — Detector Located Behind the Barrier	2
Case II — Detector Between Two Parallel Barriers	3
Case III — Detector Located Within a Box	3
Case III-A	4
Case III-B	5
Case III-C	5
RESULTS	5
DETECTOR BEHIND BARRIER	5
DETECTOR BETWEEN TWO BARRIERS	6
DETECTOR WITHIN BLOCKHOUSE	7
COMPARISON WITH EXPERIMENT	8
CONCLUSIONS	8
REFERENCES	9
APPENDIX A. DETECTOR BEHIND TWO AND THREE PARALLEL, SEPARATED BARRIERS	A-1

LIST OF ILLUSTRATIONS

<u>Figure</u>		<u>Page</u>
1	Case I — Detector Located Behind the Barrier, B	2
2	Case II — Detector Located Between Two Parallel Barriers . . .	3
3	Detector Located Within a Box	4
4	Comparison of Roof Reduction Factors Calculated by the Monte Carlo Method for Iron with that Calculated by the Moment Method for Concrete	10
5	Ratio of Dose Resulting from Slab (2) and Slab (1) for Various Separation Distances ($H/L = 1/4, 1/2, 1$) vs Solid Angle Fraction. The Mass Thickness for Each Slab was 20.5 psf . . .	11
6	Comparison of Experimental Dose with that Obtained by Monte Carlo Method Resulting from Co-60 Source at Various Angles of Incidence	12
A-1	Detector Located Behind Two Parallel Barriers	A-1
A-2	Detector Located Behind Three Parallel Barriers	A-2
A-3	Dose Due to Scattering of Photons Through Two Separated Iron Slabs, Each of Mass Thickness 20.5 psf ($H/L = 1/4, 1/2, 1$), and an Iron Slab of Mass Thickness 41.0 psf ($H/L = 0$) vs Solid Angle Fraction	A-11
A-4	Dose Due to Scattering of Photons Through Two Separated Iron Slabs, Each of Mass Thickness 20.5 psf ($H/L = 1/4, 1/2, 1$), and an Iron Slab of Mass Thickness 41.0 psf ($H/L = 0$) vs Solid Angle Fraction Subtended by the Top Barrier	A-12
A-5	Dose Due to Scattering of Photons Through Three Separated Iron Slabs of Mass Thickness 20.5 psf ($H/L:H'/L = 1/2:1/2,$ $1/2:1, 1:1/2, 1:1$) and an Iron Slab of Mass Thickness 61.5 psf ($H/L = H'/L = 0$) vs Solid Angle Fraction	A-13
A-6	Dose Due to Scattering of Photons Through Three Separated Iron Slabs of Mass Thickness 20.5 psf ($H/L:H'/L = 1/2:1/2,$ $1/2:1, 1:1/2, 1:1$) and an Iron Slab of Mass Thickness 61.5 psf ($H/L = H'/L = 0$) vs Solid Angle Fraction Subtended by the Top Barrier	A-14
A-7	Comparison of Dose Calculated by the Monte Carlo Method with that Obtained Experimentally for Normally Incident Co-60 Radiation	A-15

LIST OF TABLES

<u>Table</u>		<u>Page</u>
1	Dose Due to Scattering of Photons Through Iron Disk and Four Iron Slabs of Various Length-to-Width Ratios of Mass Thickness 20.5 psf	13
2	Dose Due to Scattering of Photons Through Iron Disk and Four Iron Slabs of Various Length-to-Width Ratios of Mass Thickness 41.0 psf	16
3	Dose Due to Scattering of Photons Through Iron Disk and Four Iron Slabs of Various Length-to-Width Ratios of Mass Thickness 61.5 psf	19
4	Roof Reduction Factors Computed by the Monte Carlo Method for 1.25 MeV Plane Isotropic Source on a Barrier of Concrete and Iron of Thickness of 61.5 psf	22
5	Dose Due to the Backscattering of Photons From the Second of Two Iron Slabs, Each of 20.5 psf Mass Thickness .	23
6	Dose Due to the Backscattering of Photons From Four Walls, Each of 20.5 psf Mass Thickness	26
7	Dose Due to the Scattering of Photons Inside a Blockhouse (Square Top and with a Ratio of H/L = 1/2 for the Height) of 20.5 psf Mass Thickness on All Sides	27
A-1	Dose Due to Scattering of Photons Through Two Iron Slabs, Each of 20.5 psf Mass Thickness	A-5
A-2	Dose Due to the Scattering of Photons Through Three Iron Slabs, Each of 20.5 psf Mass Thickness	A-8

INTRODUCTION

Monte Carlo calculational programs¹⁻⁴ currently in use at Technical Operations Research provide information regarding the reflection, absorption, and transmission of plane sources incident upon various barrier thicknesses. These programs to a greater or lesser degree consolidate the output parameters of the emergent radiation. The earlier ones yield only the polar angle of the radiation scattered out of the barrier; the more sophisticated versions add the azimuth angle, thereby doses resulting from scattered gamma rays may be estimated at various points behind (or in front of) the barrier.

The present calculational program, prepared under Contract No. OCD-OS-62-219, extends the slab geometry programs to compute the dose due to scattered photons at various positions for the following geometries:

1. One barrier of various length-to-width ratios
2. Two parallel barriers separated by various distances
(detectors between the barriers)
3. A blockhouse.

By using the results of calculations of the forward scattering and the backscattering from the single barrier geometry, we provide input source characteristics to a new geometry (e.g., barrier surrounded by five sides — blockhouse). With the exception of the blockhouse, all sources and slabs are considered to be infinite in extent, thus providing uniform spatial distributions of scattered photons behind the slab. However, the detector is assumed to respond only to radiation arriving within a solid angle corresponding to a finite slab area.

Data pertaining to geometries for detectors behind two and three parallel barriers separated by various distances are presented in the appendix of this report. As discussed in the appendix, these calculations warrant further investigation.

SCHEMATIZATION

The investigation of scattered gamma rays resulting from plane monodirectional sources on a barrier is considered for the following schematizations.

Case I — Detector Located Behind Barrier

A barrier of either circular or rectangular shape is assumed to be covered with a plane monodirectional source of gamma radiation of constant source strength per unit area. The detector is assumed to be located at various distances below the center of the barrier, as shown in Figure 1. The detector is assumed to respond only to scattered photons* having direction cosines falling within the limits set by the solid angle fraction ω (solid angle divided by 2π), subtended at the detector by the barrier. (Because of axial symmetry along the center line of the disk, the solid angle does not depend on the azimuthal angle.)

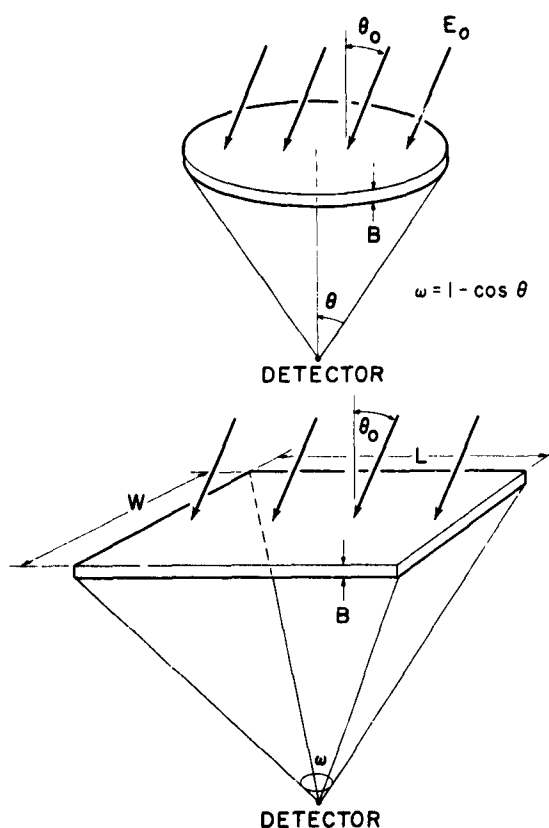


Figure 1. Case I — Detector Located Behind the Barrier, B

* In all cases considered, the detector responds only to radiation that encounters one or more collisions. The unattenuated radiation can be handled analytically.

Case II — Detector Between Two Parallel Barriers

Figure 2 shows the geometry for this case. A uniform, plane monodirectional beam of gamma photons of energy E_0 is assumed incident on the upper barrier. The detector is located between the two barriers separated by a distance H . The radiation transmitted through the top barrier is checked to determine if it will strike the bottom barrier. The photons that strike the bottom barrier are followed to determine if they are backscattered. The detector then responds to those backscattered photons that have the proper direction cosines.

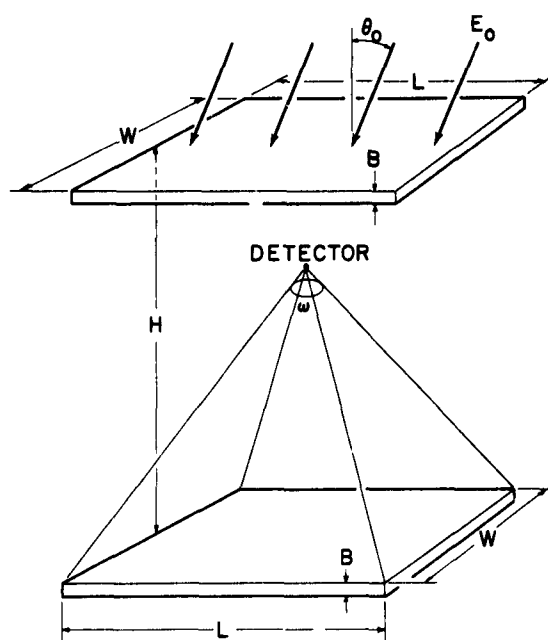


Figure 2. Case II — Detector Located Between Two Parallel Barriers

Case III — Detector Located Within a Box

A detector is placed on the center line of a box bounded by four vertical slabs and one horizontal square slab. The geometry is shown in Figure 3. The incident radiation is provided by a uniform, plane monodirectional source of energy E_0 on the horizontal slab. The detector responds to the photons that penetrated the

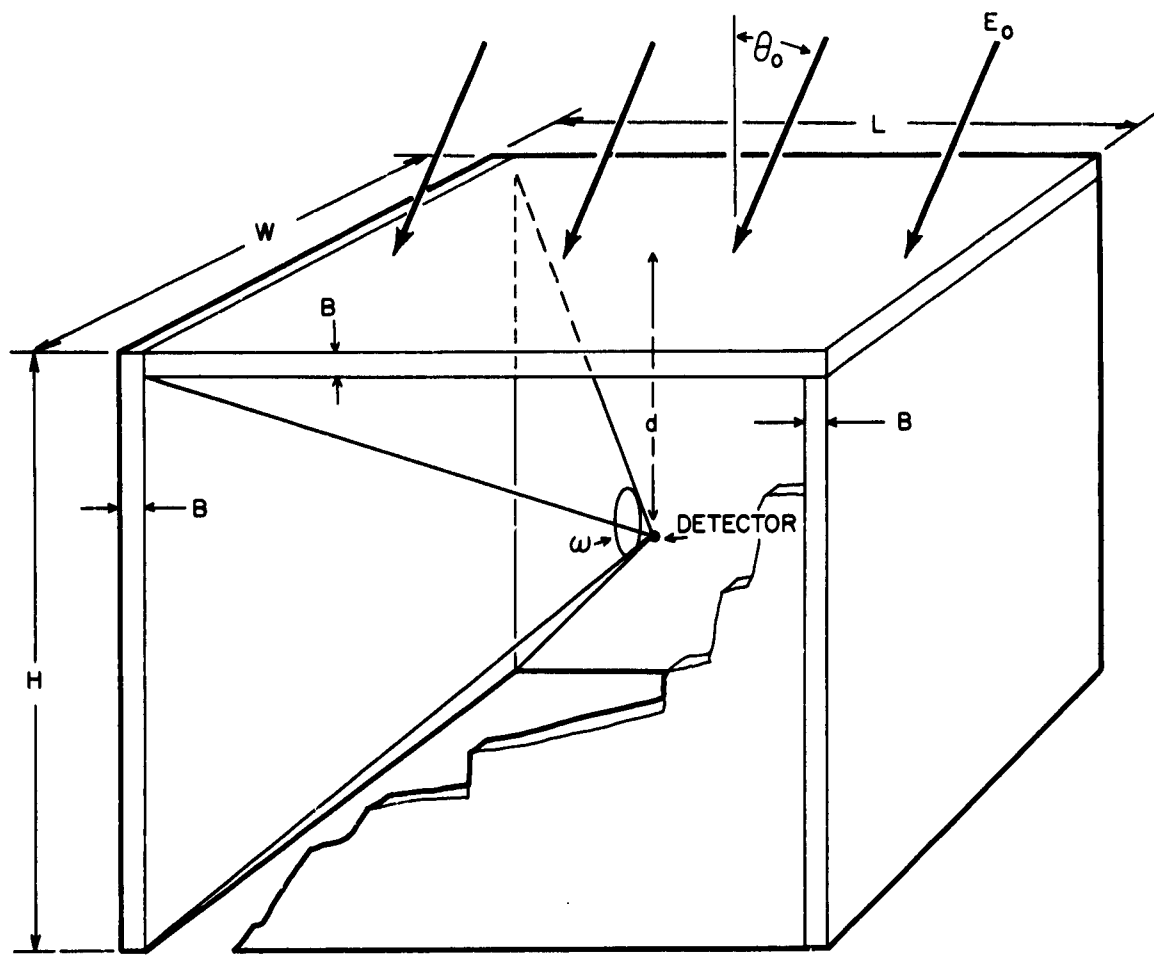


Figure 3. Detector Located Within a Box

horizontal slab and were then backscattered by the vertical barriers. The following three situations are considered:

Case III-A — Maximum Condition: All photons emerging from the ceiling are assumed to be distributed uniformly over a wall (or walls); i.e., the source density does not vary along the wall.* All photons emerging from the horizontal barrier strike the walls regardless of

*In a finite box, however, the source density along a wall is higher close to the ceiling, since the photons that emerge from the ceiling at almost grazing incidence cannot enter the bottom section of the wall.

their emergent angles. Effectively, we are considering the distribution that would result if the horizontal and vertical barriers were infinite. The photons that are backscattered from the walls and arrive at the detector are then scored.

Case III-B — Intermediate Condition: Each wall is divided into three sections of equal height. The photons emerging from the ceiling are sorted according to their emergent direction cosines to determine the section (or sections) of a wall entered. (Each section is assumed to have a uniform source density.) The photons backscattered from each section are then tested separately to compute their contribution to the detector response. This case most closely represents the physical situation.

Case III-C — Minimum Condition: The photons emerging from the ceiling are sorted to exclude all photons that would produce a nonuniform source distribution along the walls. In other words, those photons with emergent angles resulting in a higher source density distribution on the upper parts of the walls are removed. The photons that are backscattered from the walls and arrive at the detector are then scored.

RESULTS

The data in Tables 1 through 7 pertain to the dose resulting from one or more scatterings of a 1.25 MeV plane, monodirectional beam incident on iron at angles Θ_0 defined by $\cos \Theta_0 = 1.0, 0.75, 0.50, 0.25$, and 0.0 . Results were also obtained for isotropic incidence by trapezoidal integration of the monodirectional data over the angle of incidence Θ_0 . All the data are for 5000 photon histories and are given in units of keV/g, normalized to 1 incident photon/cm².

DETECTOR BEHIND BARRIER

Tables 1, 2, and 3 contain the results described in Case I for barrier thicknesses of 20.5, 41.0, and 61.5 psf, respectively. The scattered dose is given for disk barriers and for rectangular barriers of various length-to-width ratios (1.0, 1.5, 2.0, and 3.0) as a function of solid angle fraction subtended at the detector. It is evident that the scattered dose is almost independent of barrier shape.

Spencer⁵ used the moment method to determine the amount of protection provided by various concretelike structures from fallout radiation (assuming the spectrum at 1.12 hr after fission) and from two monoenergetic sources (1.25 and 0.66 MeV) on the ground and on the roof. His results are given in terms of reduction factors that are defined as follows: The ratio of the detector response (from the sources on the ground and/or the sources on the roof) in a protected position to the detector response 3 ft above an infinite plane uniformly contaminated with the same source density. The term $L(X) L_a(X, \omega)$ given by Spencer is the attenuation of radiation from an infinite, plane isotropic source in an infinite medium as a function of barrier thickness and solid angle fraction. The present Monte Carlo calculation assumes a barrier with the source on one side and in a vacuum. Therefore, to compare these two methods, the contribution from radiation which resembles skyshine should be subtracted from Spencer's infinite medium results. This radiation originates at the source plane, is backscattered in the infinite medium behind the barrier and, penetrating the barrier, arrives at the detector within the solid angle fraction ω . In Spencer's terms this radiation is given by $S(d) S_a(d, \omega) S'(X)$. Figure 4 shows the modified roof reduction factors for a Co-60, plane isotropic source on disk barriers of 20.5, 41.0, and 61.5 psf thicknesses of iron. The abscissa is in units of solid angle fraction $\omega = 1 - \cos \Theta$. Although the present Monte Carlo results were obtained for barriers of iron, comparisons with Spencer's roof reduction factors are valid, since, for the thicknesses considered, iron and concretelike materials have similar scattering properties. To substantiate this point, Table 4 gives roof reduction factors for the two materials at a thickness of 61.5 psf. The concrete data in the table were obtained by a previous calculation.² Note that since the source on the top of the disk is isotropic and is uniformly distributed, the photons scattered through the disk will also be uniformly distributed, and the azimuthal variable can be integrated out. The two methods are in good agreement.

DETECTOR BETWEEN TWO BARRIERS

Table 5 gives the results for the geometry described in Case II, where the detector is located between two barriers of 20.5 psf. The dose backscattered by the lower slab is given as a function of solid angle fraction and three separation distances ($H/L = 1/4, 1/2, \text{ and } 1$). The data in the table indicate that for normal incidence the dose does not vary significantly with separation distances; i. e., the photons transmitted by the top barrier are primarily traveling in the forward direction.

Figure 5 shows the effect of having a 1.25 MeV plane isotropic source on one slab and the detector between two slabs of equal thickness with various separation distances. The figure shows the ratio of the backscattered dose resulting from slab (2) to the scattered dose from slab (1) as a function of solid angle fraction, ω , measured with respect to slab (1). The backscattered dose from slab (2) is the result of all radiation that originally had struck slab (2) and then backscattered. The dose due to the backscattered radiation from slab (2) can be as high as 60% of the transmitted scattered radiation through slab (1) depending upon the separation distance and the location of the detector. The closer the detector is to slab (2), the higher the contribution from slab (2).

DETECTOR WITHIN A BLOCKHOUSE

Table 6 contains the results described in Case III where a 1.25 MeV plane source is incident on the horizontal iron slab at various angles ($\cos \Theta_0 = 1.0, 0.75, 0.50, 0.25, \text{ and } 0.00$, and isotropic incidence). The barrier thickness is 20.5 psf on each side, and the ratio of the height of the vertical slab to the length of the horizontal slab H/L is $1/2$. Three detector locations along the vertical center line are indicated by three values of d/L (distance from the detector to the ceiling/length of horizontal slab) $0.08333, 0.25, \text{ and } 0.41667$. For each detector position, tabulations are made of the dose resulting from backscattering from the walls for each of the three cases A, B, and C given in Case III. The results of cases A, B, and C do not vary significantly for a given $\cos \Theta_0$, and detector response due to the walls increases as the detector position is lowered.

By combining Cases I, II, and III, we may estimate the total dose inside a blockhouse. The contributions to the detector include:

1. Photons passing unattenuated through the blockhouse roof
2. Photons scattered by the blockhouse roof
3. Both scattered and unattenuated photons traversing the blockhouse roof, entering one of the sides or the bottom, and then re-emerging into the blockhouse.

All other possible paths that a photon may trace are ignored; for example, photons penetrating the roof, entering the floor, re-emerging, entering a side, and finally reaching the detector.

Table 7 contains the dose (column 5) in a blockhouse (barrier thickness of 20.5 psf) for the detector positions corresponding to the three values of d/L found in Table 8 (the effect of the side walls). Also given in Table 9 are the doses for each of the radiating plane sources. Column 2 contains the dose due to the scattered photons through the top barrier (Case I); column 3 contains the dose backscattered from the floor (Case II); and column 4 contains the dose backscattered from the side walls (Case III-B). The data in the table indicate that the dose resulting from the side walls and floor becomes increasingly significant as the detector approaches the lower portion of the blockhouse. It may also be noted that the backscattered contribution from the floor would be further increased if the floor were thicker.

COMPARISON WITH EXPERIMENT

Experiments described in detail elsewhere⁶ were performed at Tech/Ops to measure doses due to scattered photons resulting from Co-60 radiation on iron slabs. The pertinent results of these experiments are presented in Figure 6 along with results of Monte Carlo calculations for comparison. Figure 6 shows the results of an experiment in which three detectors were placed behind the first of four iron slabs. The slabs, spaced 1 ft apart, are each 2 ft x 2 ft and 41.0 psf thick. The detectors are placed 2 in., 6 in., and 10 in. behind the center of the first slab, as shown in Figures 6a, 6b, and 6c, respectively. A Co-60, plane parallel beam is incident on the first slab at five angles of incidence ($\theta_o = 15^\circ, 30^\circ, 45^\circ, 60^\circ, \text{ and } 75^\circ$). The experimental results (circles) are compared with curves obtained from Monte Carlo calculations on a single slab between source and detector (Case I).

CONCLUSIONS

The results from the Monte Carlo calculations indicate that the following conclusions may be drawn:

1. The dose along the center line behind the barrier for a given solid angle is essentially the same, regardless of the shape of the barrier (circular or rectangular). For the geometries investigated, there was practically no variation in dose with barrier eccentricity.

2. When the detector is placed between two barriers, the dose resulting from radiation backscattered by the floor may be significant if the detector is near the floor.

3. When the detector is surrounded by four vertical walls, the detector response due to the vertical walls is essentially the same whether one considers the distribution of radiation resulting from infinite walls or finite walls.

REFERENCES

1. M. J. Berger and D. J. Raso, "Monte Carlo Calculations of Gamma-Ray Backscattering," *Radiation Research* 12, 20-37 (1960).
2. D. J. Raso, "Transmission of Scattered Gamma Rays Through Concrete and Iron Slabs," *Health Physics* 5, 126-141 (1961).
3. D. J. Raso, "Scattering of X-Rays in Laminar Media," *Radiation Research* 19, 384-391 (1963).
4. D. J. Raso, "Monte Carlo Calculations on the Reflection and Transmission of Scattered Gamma Radiations," *J. Nuclear Science and Engineering* 17, 411-418 (1963).
5. L. V. Spencer, "Structure Shielding Against Fallout Radiation from Nuclear Weapons," *National Bureau of Standards Monograph* 42 (1962).
6. M. J. Barrett and R. L. MacNeil, "Dose Rate Distribution in a Compartmented Structure," *Technical Operations Research*, Report TO-B 64-1 (June, 1964).

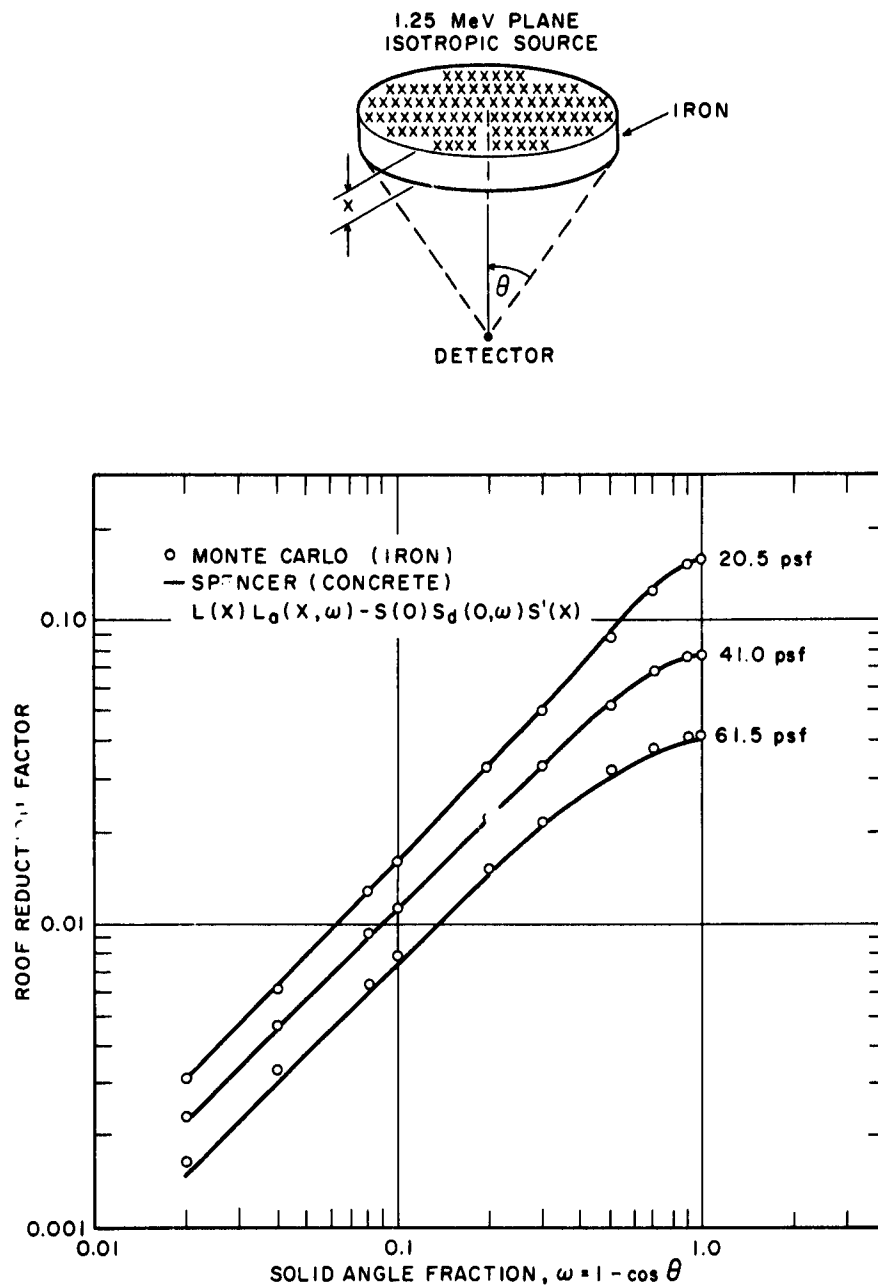


Figure 4. Comparison of Roof Reduction Factors Calculated by the Monte Carlo Method for Iron with that Calculated by the Moment Method for Concrete

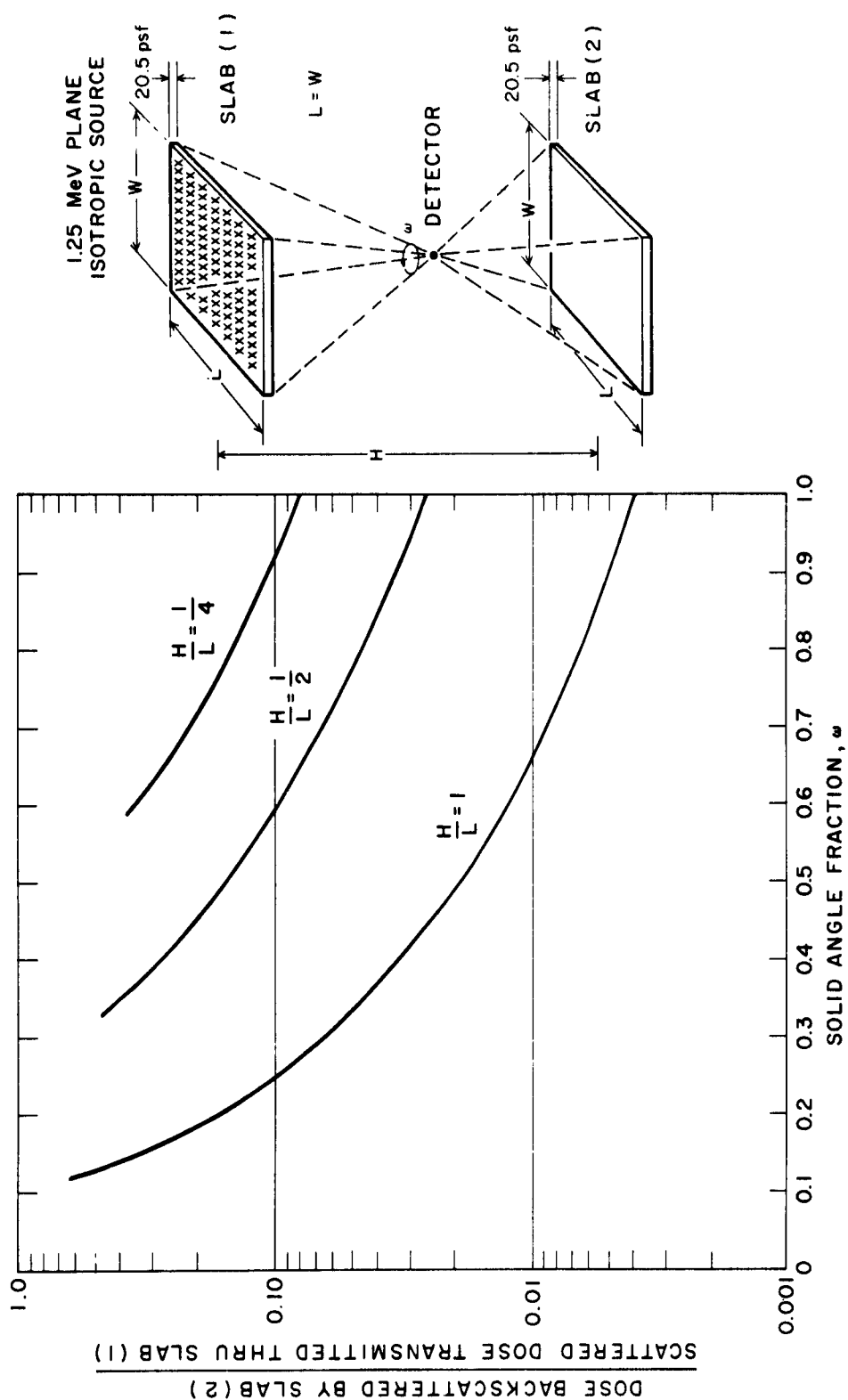


Figure 5. Ratio of Dose Resulting from Slab (2) and Slab (1) for Various Separation Distances ($H/L = 1/4, 1/2, 1$) vs Solid Angle Fraction. The Mass Thickness for Each Slab was 20.5 psf

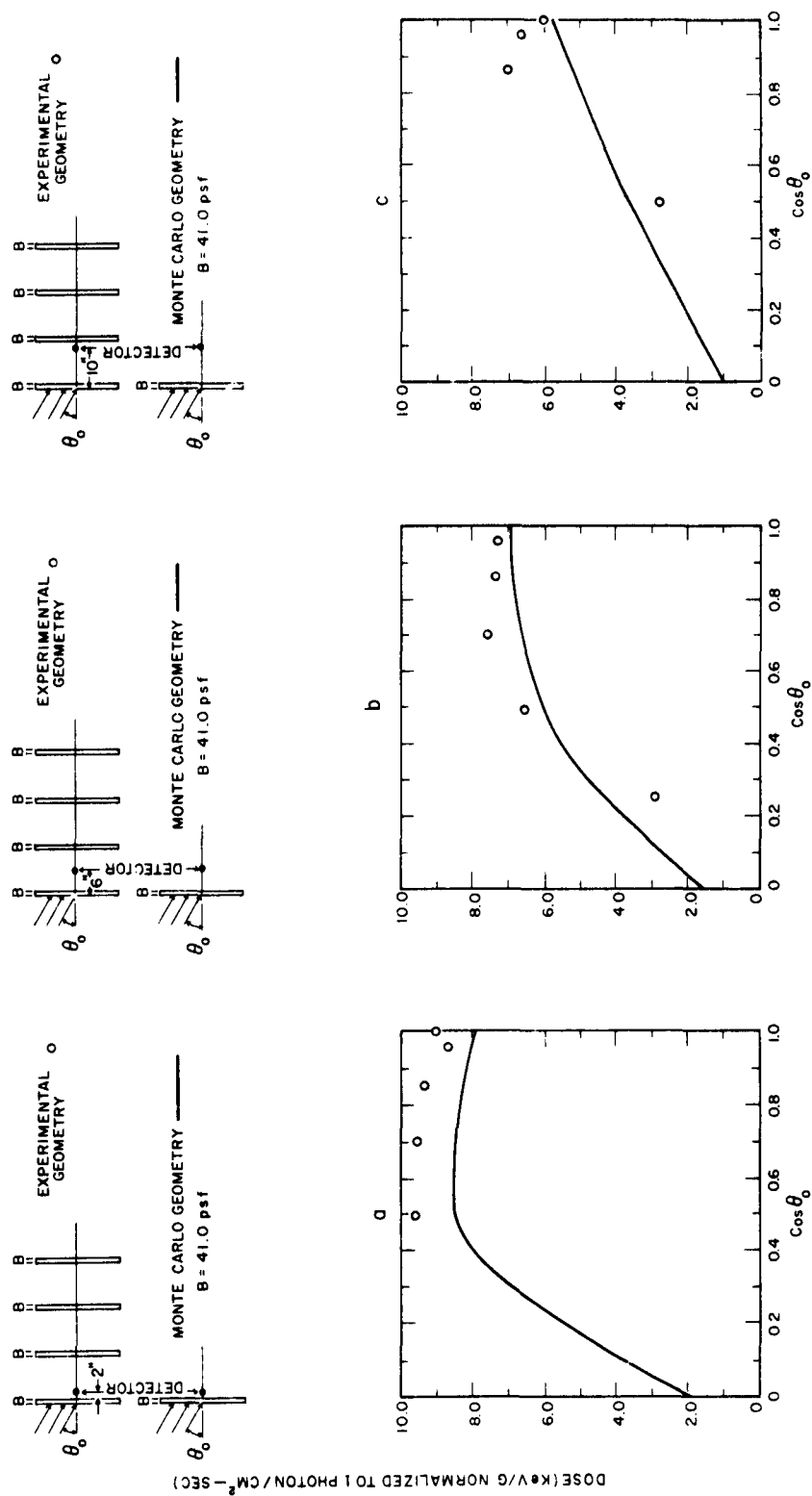


Figure 6. Comparison of Experimental Dose with that Obtained by Monte Carlo Method Resulting from Co-60 Source at Various Angles of Incidence

TABLE 1
DOSE DUE TO SCATTERING OF PHOTONS THROUGH IRON DISK AND
FOUR IRON SLABS OF VARIOUS LENGTH-TO-WIDTH RATIOS
OF MASS THICKNESS 20.5 psi^{*†}

(KeV/g normalized to 1 photon/cm²)

ω	Disk	L = W	L = 1.5 W	L = 2.0 W	L = 3.0 W
$\cos \Theta_o = 1.0$					
0.02	0.465	0.478	0.491	0.450	0.438
0.04	0.902	0.953	0.919	0.855	0.830
0.08	1.74	1.69	1.60	1.56	1.51
0.10	2.13	2.07	1.93	1.89	1.79
0.20	3.34	3.37	3.26	3.22	3.04
0.30	4.24	4.29	4.18	4.04	3.94
0.50	5.57	5.54	5.53	5.53	5.41
0.70	6.44	6.46	6.45	6.44	6.38
0.90	7.04	7.02	7.04	7.04	7.04
1.00	7.35	7.35	7.35	7.35	7.35
$\cos \Theta_o = 0.75$					
0.02	0.210	0.214	0.196	0.211	0.196
0.04	0.340	0.346	0.376	0.379	0.394
0.08	0.858	0.864	0.714	0.663	0.738
0.10	1.08	1.09	0.934	0.926	0.872
0.20	2.26	2.27	2.02	1.83	1.73
0.30	3.51	3.43	3.06	2.87	2.64
0.50	5.05	5.62	5.16	5.05	4.92
0.70	7.86	7.80	7.65	7.53	7.40
0.90	9.54	9.54	9.36	9.34	9.39
1.00	10.5	10.5	10.5	10.5	10.5

* 5000 photons of energy 1.25 MeV are assumed incident on the barriers with angles for each of the five cases given by $\cos \Theta_o = 1.0, 0.75, 0.50, 0.25$, and 0.00.

† Results for isotropic incidence are obtained by integration of the monodirectional data.

TABLE 1 (Cont'd.)
DOSE DUE TO SCATTERING OF PHOTONS THROUGH IRON DISK AND
FOUR IRON SLABS OF VARIOUS LENGTH-TO-WIDTH RATIOS
OF MASS THICKNESS 20.5 psf
(KeV/g normalized to 1 photon/cm²)

ω	Disk	L = W	L = 1.5 W	L = 2.0 W	L = 3.0 W
$\cos \theta_o = 0.50$					
0.02	0.0965	0.104	0.117	0.130	0.121
0.04	0.253	0.272	0.257	0.244	0.250
0.08	0.562	0.574	0.542	0.531	0.473
0.10	0.728	0.731	0.654	0.671	0.656
0.20	1.60	1.60	1.40	1.35	1.28
0.30	2.70	2.58	2.29	2.17	2.07
0.50	5.46	5.38	4.63	4.45	4.23
0.70	8.84	8.62	8.22	8.11	7.81
0.90	11.7	11.6	11.5	11.5	11.5
1.00	12.4	12.4	12.4	12.4	12.4
$\cos \theta_o = 0.25$					
0.02	0.119	0.116	0.111	0.114	0.105
0.04	0.221	0.228	0.237	0.218	0.217
0.08	0.461	0.449	0.441	0.420	0.408
0.10	0.579	0.585	0.540	0.544	0.505
0.20	1.29	1.33	1.22	1.13	1.12
0.30	2.15	2.17	1.96	1.94	1.88
0.50	4.99	4.72	4.16	4.03	3.81
0.70	9.04	8.73	8.18	7.90	7.61
0.90	13.1	12.9	12.8	12.7	12.7
1.00	14.3	14.3	14.3	14.3	14.3

TABLE 1 (Cont'd.)
DOSE DUE TO SCATTERING OF PHOTONS THROUGH IRON DISK AND
FOUR IRON SLABS OF VARIOUS LENGTH-TO-WIDTH RATIOS
OF MASS THICKNESS 20.5 psf
(Kev/g normalized to 1 photon/cm²)

ω	Disk	L = W	L = 1.5 W	L = 2.0 W	L = 3.0 W
Cos $\Theta_0 = 0.0$					
0.02	0.0602	0.0638	0.060	0.0563	0.0699
0.04	0.106	0.114	0.108	0.104	0.116
0.08	0.267	0.251	0.253	0.249	0.241
0.10	0.340	0.338	0.324	0.342	0.319
0.20	0.806	0.784	0.718	0.670	0.674
0.30	1.27	1.33	1.23	1.19	1.17
0.50	2.76	2.73	2.42	2.38	2.28
0.70	4.39	4.36	4.05	3.93	3.85
0.90	5.74	5.69	5.66	5.66	5.66
1.00	5.82	5.82	5.82	5.82	5.82
Isotropic					
0.02	0.172	0.176	0.175	0.177	0.169
0.04	0.329	0.345	0.346	0.330	0.334
0.08	0.721	0.715	0.655	0.629	0.623
0.10	0.905	0.902	0.814	0.815	0.772
0.20	1.80	1.82	1.66	1.56	1.50
0.30	2.78	2.75	2.50	2.40	2.29
0.50	5.07	4.96	4.48	4.37	4.20
0.70	7.79	7.64	7.32	7.18	6.98
0.90	10.2	10.1	10.0	9.96	9.98
1.00	10.9	10.9	10.9	10.9	10.9

TABLE 2
DOSE DUE TO SCATTERING OF PHOTONS THROUGH IRON DISK AND
FOUR IRON SLABS OF VARIOUS LENGTH-TO-WIDTH RATIOS
OF MASS THICKNESS 41.0 psf*†

(KeV/g normalized to 1 photon/cm²)

ω	Disk	L = W	L = 1.5 W	L = 2.0 W	L = 3.0 W
Cos $\Theta_0 = 1.0$					
0.02	0.597	0.568	0.646	0.635	0.599
0.04	1.18	1.27	1.17	1.10	1.17
0.08	2.15	2.09	2.05	2.10	2.05
0.10	2.61	2.54	2.49	2.49	2.39
0.20	4.17	4.19	4.06	3.98	3.78
0.30	5.17	5.14	5.09	5.00	4.90
0.50	6.52	6.47	6.47	6.50	6.46
0.70	7.53	7.50	7.55	7.55	7.48
0.90	8.04	8.04	8.03	8.03	8.05
1.00	8.32	8.32	8.32	8.32	8.32
Cos $\Theta_0 = 0.75$					
0.02	0.281	0.288	0.282	0.293	0.252
0.04	0.469	0.504	0.510	0.482	0.486
0.08	0.962	1.01	0.879	0.837	0.841
0.10	1.20	1.23	1.12	1.08	1.04
0.20	2.54	2.55	2.16	2.00	1.96
0.30	3.86	3.75	3.43	3.23	2.97
0.50	6.07	5.96	5.57	5.46	5.29
0.70	7.58	7.55	7.52	7.34	7.21
0.90	8.69	8.64	8.58	8.55	8.58
1.00	8.92	8.92	8.92	8.92	8.92

* 5000 photons of energy 1.25 MeV are assumed incident on the barriers with angles for each of the five cases given by cos $\Theta_0 = 1.0, 0.75, 0.50, 0.25,$ and 0.00.

† Results for isotropic incidence are obtained by integration of the monodirectional data.

TABLE 2 (Cont'd.)
 DOSE DUE TO SCATTERING OF PHOTONS THROUGH IRON DISK AND
 FOUR IRON SLABS OF VARIOUS LENGTH-TO-WIDTH RATIOS
 OF MASS THICKNESS 41.0 psf
 (KeV/g normalized to 1 photon/cm²)

ω	Disk	L = W	L = 1.5 W	L = 2.0 W	L = 3.0 W
$\cos \theta_0 = 0.50$					
0.02	0.114	0.125	0.116	0.129	0.116
0.04	0.272	0.287	0.265	0.252	0.262
0.08	0.608	0.608	0.539	0.548	0.519
0.10	0.777	0.744	0.712	0.707	0.659
0.20	1.69	1.70	1.44	1.39	1.32
0.30	2.80	2.62	2.40	2.23	2.12
0.50	5.13	5.02	4.42	4.28	4.09
0.70	7.35	7.25	7.00	6.87	6.70
0.90	8.98	8.87	8.78	8.78	8.87
1.00	9.21	9.21	9.21	9.21	9.21
$\cos \theta_0 = 0.25$					
0.02	0.0936	0.0884	0.0879	0.0969	0.108
0.04	0.202	0.201	0.209	0.187	0.182
0.08	0.398	0.411	0.378	0.341	0.346
0.10	0.500	0.510	0.472	0.458	0.426
0.20	1.07	1.13	0.969	0.898	0.860
0.30	1.69	1.71	1.53	1.49	1.36
0.50	3.31	3.21	2.88	2.70	2.62
0.70	5.28	5.29	4.94	4.83	4.62
0.90	6.56	6.56	6.50	6.45	6.65
1.00	6.77	6.77	6.77	6.77	6.77

TABLE 2 (Cont'd.)
DOSE DUE TO SCATTERING OF PHOTONS THROUGH IRON DISK AND
FOUR IRON SLABS OF VARIOUS LENGTH-TO-WIDTH RATIOS
OF MASS THICKNESS 41.0 psf
(KeV/g normalized to 1 photon/cm²)

ω	Disk	L = W	L = 1.5 W	L = 2.0 W	L = 3.0 W
Cos $\theta_0 = 0.0$					
0.02	0.0424	0.0491	0.0452	0.0398	0.0469
0.04	0.0708	0.0812	0.0771	0.0769	0.0901
0.08	0.187	0.180	0.183	0.156	0.137
0.10	0.237	0.232	0.213	0.214	0.187
0.20	0.423	0.420	0.425	0.405	0.396
0.30	0.705	0.714	0.658	0.616	0.619
0.50	1.36	1.35	1.26	1.21	1.14
0.70	1.89	1.88	1.80	1.79	1.78
0.90	2.15	2.15	2.15	2.15	2.18
1.00	2.18	2.18	2.18	2.18	2.18
Isotropic					
0.02	0.202	0.203	0.208	0.214	0.200
0.04	0.391	0.417	0.402	0.378	0.390
0.08	0.783	0.790	0.728	0.713	0.700
0.10	0.974	0.966	0.913	0.899	0.853
0.20	1.89	1.92	1.70	1.62	1.56
0.30	2.82	2.75	2.56	2.44	2.30
0.50	4.59	4.53	4.18	4.07	3.95
0.70	6.23	6.19	6.03	5.93	5.79
0.90	7.33	7.29	7.24	7.22	7.30
1.00	7.54	7.54	7.54	7.54	7.54

TABLE 3
DOSE DUE TO SCATTERING OF PHOTONS THROUGH IRON DISK AND
FOUR IRON SLABS OF VARIOUS LENGTH-TO-WIDTH RATIOS
OF MASS THICKNESS 61.5 psf*†

(KeV/g normalized to 1 photon/cm²)

ω	Disk	L = W	L = 1.5 W	L = 2.0 W	L = 3.0 W
$\cos \Theta_0 = 1.0$					
0.02	0.523	0.475	0.549	0.536	0.509
0.04	0.970	1.03	0.976	0.935	0.955
0.08	1.84	1.78	1.72	1.69	1.70
0.10	2.25	2.24	2.12	2.12	2.00
0.20	3.76	3.73	3.64	3.57	3.39
0.30	4.69	4.76	4.63	4.58	4.44
0.50	5.86	5.88	5.87	5.89	5.89
0.70	6.67	6.66	6.71	6.68	6.65
0.90	7.05	7.05	7.05	7.05	7.05
1.00	7.20	7.20	7.20	7.20	7.20
$\cos \Theta_0 = 0.75$					
0.02	0.283	0.267	0.274	0.277	0.243
0.04	0.520	0.529	0.519	0.476	0.467
0.08	0.922	0.955	0.859	0.831	0.843
0.10	1.13	1.19	1.06	1.04	0.988
0.20	2.27	2.31	1.93	1.85	1.80
0.30	3.37	3.25	2.99	2.86	2.63
0.50	5.07	4.96	4.62	4.55	4.49
0.70	6.10	6.07	6.07	6.01	5.89
0.90	6.61	6.61	6.61	6.61	6.67
1.00	6.83	6.83	6.83	6.83	6.83

* 5000 photons of energy 1.25 MeV are assumed incident on the barriers with angles for each of the five cases given by $\cos \Theta_0 = 1.0, 0.75, 0.50, 0.25$, and 0.00.

† Results for isotropic incidence are obtained by integration of the monodirectional data.

TABLE 3 (Cont'd.)
DOSE DUE TO SCATTERING OF PHOTONS THROUGH IRON DISK AND
FOUR IRON SLABS OF VARIOUS LENGTH-TO-WIDTH RATIOS
OF MASS THICKNESS 61.5 psf
(KeV/g normalized to 1 photon/cm²)

ω	Disk	L = W	L = 1.5 W	L = 2.0 W	L = 3.0 W
$\text{Cos } \Theta_0 = 0.50$					
0.02	0.0913	0.0995	0.0802	0.0806	0.0892
0.04	0.187	0.188	0.175	0.169	0.155
0.08	0.412	0.423	0.367	0.347	0.321
0.10	0.556	0.507	0.482	0.477	0.397
0.20	1.10	1.13	0.969	0.961	0.903
0.30	1.85	1.77	1.60	1.52	1.40
0.50	3.10	3.07	2.73	2.70	2.56
0.70	4.26	4.28	4.18	4.10	4.04
0.90	4.93	4.92	4.89	4.89	4.99
1.00	5.13	5.13	5.13	5.13	5.13
$\text{Cos } \Theta_0 = 0.25$					
0.02	0.0543	0.0550	0.0461	0.0571	0.0695
0.04	0.124	0.115	0.138	0.124	0.105
0.08	0.225	0.242	0.217	0.211	0.200
0.10	0.286	0.301	0.275	0.267	0.260
0.20	0.603	0.619	0.571	0.571	0.559
0.30	1.01	1.02	0.937	0.870	0.831
0.50	1.78	1.68	1.57	1.51	1.47
0.70	2.45	2.48	2.42	2.37	2.31
0.90	2.92	2.92	2.92	2.92	2.92
1.00	2.94	2.94	2.94	2.94	2.94

TABLE 3 (Cont'd)
 DOSE DUE TO SCATTERING OF PHOTONS THROUGH IRON DISK AND
 FOUR IRON SLABS OF VARIOUS LENGTH-TO-WIDTH RATIOS
 OF MASS THICKNESS 61.5 psf
 (KeV/g normalized to 1 photon/cm²)

ω	Disk	L = W	L = 1.5 W	L = 2.0 W	L = 3.0 W
Cos $\Theta_0 = 0.00$					
0.02	0.0302	0.0364	0.0319	0.0284	0.030
0.04	0.0471	0.0516	0.0523	0.0551	0.0642
0.08	0.116	0.106	0.116	0.108	0.0956
0.10	0.146	0.147	0.138	0.138	0.116
0.20	0.242	0.228	0.232	0.237	0.247
0.30	0.360	0.344	0.315	0.303	0.306
0.50	0.630	0.615	0.574	0.563	0.542
0.70	0.815	0.796	0.747	0.753	0.742
0.90	0.863	0.858	0.858	0.858	0.881
1.00	0.906	0.906	0.906	0.906	0.906
Isotropic					
0.02	0.176	0.169	0.173	0.174	0.168
0.04	0.335	0.343	0.337	0.316	0.309
0.03	0.634	0.641	0.590	0.573	0.565
0.10	0.792	0.796	0.735	0.729	0.676
0.20	1.49	1.51	1.35	1.32	1.27
0.30	2.19	2.15	2.00	1.92	1.81
0.50	3.30	3.24	3.04	2.99	2.93
0.70	4.14	4.14	4.10	4.05	3.98
0.90	4.60	4.60	4.59	4.59	4.64
1.00	4.74	4.74	4.74	4.74	4.74

TABLE 4
 ROOF REDUCTION FACTORS COMPUTED BY
 THE MONTE CARLO METHOD FOR 1.25 MeV PLANE
 ISOTROPIC SOURCE ON A BARRIER OF CONCRETE AND
 IRON OF THICKNESS OF 61.5 psf

ω	Concrete *	Iron
0.02	0.0014	0.0016
0.04	0.0030	0.0033
0.08	0.0063	0.0064
0.10	0.0079	0.0079
0.20	0.0150	0.0150
0.30	0.0212	0.0217
0.50	0.0310	0.0320
0.70	0.0365	0.0383
0.90	0.0410	0.0410
1.00	0.0419	0.0418

* D. J. Raso "Transmission of Scattered Gamma Rays Through Concrete and Iron Slabs," Health Physics 5, 126-141 (1961).

TABLE 5

DOSE DUE TO THE BACKSCATTERING OF PHOTONS FROM THE
SECOND OF TWO IRON SLABS, EACH OF 20.5 psf MASS THICKNESS*†
(KeV/g normalized to 1 photon/cm²)

ω \ H/L [‡]	1	$\frac{1}{2}$	$\frac{1}{4}$	1	$\frac{1}{2}$	$\frac{1}{4}$
	Cos $\Theta_0 = 1.0$			Cos $\Theta_0 = 0.75$		
0.12833	0.0849			0.0831		
0.13888	0.0915			0.0929		
0.15166	0.101			0.103		
0.16555	0.109			0.114		
0.18111	0.102			0.148		
0.19888	0.134			0.171		
0.21944	0.138			0.179		
0.24222	0.155			0.201		
0.26888	0.170			0.229		
0.33333	0.229	0.269		0.313	0.383	
0.37277	0.274	0.323		0.363	0.441	
0.41744	0.318	0.380		0.415	0.505	
0.46833	0.386	0.453		0.487	0.590	
0.52611	0.428	0.512		0.571	0.692	
0.59055	0.504	0.598	0.625	0.680	0.818	0.898
0.66166	0.617	0.727	0.766	0.851	1.01	1.12
0.73944	0.745	0.876	0.917	0.953	1.14	1.27
0.82277	0.853	0.998	1.05	1.09	1.30	1.47
0.91033	0.941	1.11	1.17	1.36	1.63	1.87
1.00000	1.09	1.26	1.33	1.66	1.95	2.27

* 5000 photons of energy 1.25 MeV are assumed incident on the first slab with angles for each of the five cases given by $\cos \Theta_0 = 1.0, 0.75, 0.50, 0.25$, and 0.00 .

† Results for isotropic incidence are obtained by integration of the monodirectional data.

‡ H/L gives slab separations (ratio of separation distance to length of slab).

TABLE 5 (Cont'd.)

DOSE DUE TO THE BACKSCATTERING OF PHOTONS FROM THE
SECOND OF TWO IRON SLABS, EACH OF 20.5 psf MASS THICKNESS
(Kev/g normalized to 1 photon/cm²)

ω \ H/L	1	$\frac{1}{2}$	$\frac{1}{4}$	1	$\frac{1}{2}$	$\frac{1}{4}$
	$\cos \theta_o = 0.50$			$\cos \theta_o = 0.25$		
0.12833	0.0185			0.0208		
0.13888	0.0199			0.0208		
0.15166	0.0262			0.0219		
0.16555	0.0303			0.0263		
0.18111	0.0369			0.0270		
0.19888	0.0399			0.0318		
0.21944	0.0465			0.0339		
0.24222	0.0520			0.0375		
0.26888	0.0567			0.0461		
0.33333	0.0606	0.442		0.0531	0.140	
0.37277	0.0804	0.519		0.0568	0.167	
0.41744	0.0939	0.632		0.0678	0.191	
0.46833	0.100	0.687		0.0745	0.207	
0.52611	0.116	0.843		0.0849	0.250	
0.59055	0.131	0.967	1.14	0.103	0.292	0.801
0.66166	0.157	1.18	1.37	0.115	0.369	0.996
0.73944	0.170	1.36	1.58	0.143	0.437	1.26
0.82277	0.196	1.59	1.87	0.165	0.537	1.65
0.91033	0.233	1.94	2.22	0.223	0.667	2.09
1.00000	0.233	2.33	2.78	0.274	0.768	2.99

TABLE 5 (Cont'd.)

DOSE DUE TO THE BACKSCATTERING OF PHOTONS FROM THE
SECOND OF TWO IRON SLABS, EACH OF 20.5 psf MASS THICKNESS
(KeV/g normalized to 1 photon/cm²)

ω \ H/L	1	$\frac{1}{2}$	$\frac{1}{4}$	1	$\frac{1}{2}$	$\frac{1}{4}$
	Cos $\Theta_0 = 0.00$			Isotropic		
0.12833	0.00836			0.0423		
0.13888	0.0104			0.0461		
0.15166	0.0104			0.0518		
0.16555	0.0116			0.0576		
0.18111	0.0148			0.0697		
0.19888	0.0152			0.0793		
0.21944	0.0196			0.0846		
0.24222	0.0264			0.0953		
0.26888	0.0318			0.108		
0.33333	0.0374	0.0736		0.140	0.284	
0.37277	0.0417	0.0850		0.164	0.333	
0.41744	0.0496	0.0946		0.190	0.391	
0.46833	0.0654	0.129		0.222	0.444	
0.52611	0.0744	0.144		0.256	0.528	
0.59055	0.0826	0.163	0.216	0.302	0.614	0.878
0.66166	0.0981	0.214	0.277	0.370	0.756	1.00
0.73944	0.117	0.252	0.317	0.424	0.874	1.18
0.82277	0.124	0.278	0.352	0.485	1.02	1.42
0.91033	0.131	0.301	0.411	0.587	1.23	1.74
1.00000	0.158	0.329	0.537	0.699	1.46	2.24

TABLE 6
DOSE DUE TO THE BACKSCATTERING OF PHOTONS FROM
FOUR WALLS, EACH OF 20.5 psf MASS THICKNESS
(KeV/g normalized to 1 photon/cm²)

$\cos \theta_0^*$	Case A	Case B	Case C	Case A	Case B	Case C
	Detector Position (d/L = 0.08333) ‡			Detector Position (d/L = 0.25)		
1.0	1.87	1.87	1.85	2.02	2.02	2.00
0.75	0.876	0.872	0.844	1.08	1.07	1.04
0.50	0.665	0.657	0.621	0.829	0.820	0.764
0.25	0.380	0.348	0.230	0.494	0.447	0.288
0.00	0.166	0.166	0.145	0.169	0.164	0.143
Isotropic†	0.735	0.724	0.674	0.874	0.858	0.791
	Detector Position (d/L = 0.41667)			<p>* 5000 photons of energy 1.25 MeV are assumed incident on the top slab with angles for each of the five cases given by $\cos \theta_0 = 1.0, 0.75, 0.50, 0.25$, and 0.00.</p> <p>† Results for isotropic incidence are obtained by integration of the monodirectional data.</p> <p>‡ d/L is the ratio of the distance of the detector from the top slab to the length of a horizontal slab.</p>		
1.0	1.89	1.89	1.87			
0.75	1.23	1.22	1.19			
0.50	0.955	0.948	0.884			
0.25	0.550	0.494	0.287			
0.00	0.163	0.161	0.137			
Isotropic	0.941	0.922	0.842			

TABLE 7

DOSE DUE TO THE SCATTERING OF PHOTONS INSIDE A BLOCKHOUSE
(SQUARE TOP AND WITH A RATIO OF $H/L = 1/2$ FOR THE HEIGHT)
OF 20.5 psf MASS THICKNESS ON ALL SIDES

(Kev/g normalized to 1 photon/cm²)

$\cos \theta_o^*$	Scattered Through Top Barrier	Backscattered From Floor	Backscattered From Side Walls	Total
	Detector Position (d/L = 0.08333)†			
1.0	6.88	0.341	1.87	9.09
0.75	9.11	0.462	0.872	10.4
0.50	10.9	0.555	0.657	12.1
0.25	11.9	0.174	0.348	12.4
0.00	5.37	0.088	0.166	5.62
Isotropic‡	9.51	0.351	0.724	10.6
	Detector Position (d/L = 0.25)			
1.0	6.09	0.598	2.02	8.71
0.75	6.60	0.818	1.07	8.49
0.50	6.84	0.967	0.820	8.63
0.25	6.54	0.292	0.447	7.28
0.00	3.47	0.163	0.164	3.80
Isotropic	6.19	0.614	0.858	7.66
	Detector Position (d/L = 0.41667)			
1.0	4.84	1.033	1.89	7.76
0.75	4.38	1.41	1.22	7.01
0.50	3.80	1.70	0.948	6.45
0.25	3.28	0.579	0.494	4.35
0.00	1.94	0.285	0.161	2.39
Isotropic	3.71	1.09	0.922	5.72

* 5000 photons of energy 1.25 MeV are assumed incident on the roof with angles for each of the five cases of incidence given by $\cos \theta_o = 1.0, 0.75, 0.50, 0.25$, and 0.00.

† d/L is the ratio of the distance of the detector from the roof to the roof length.

‡ Results for isotropic incidence are obtained by integration of the monodirectional data.

APPENDIX A

DETECTOR BEHIND TWO AND THREE PARALLEL
SEPARATED BARRIERS

The following results have been obtained for the assumption of uniform illumination on a bottom slab from radiation emanating from a finite portion of an infinite top barrier. This approach might very well be considered to yield an overestimate of the actual (finite) barrier case. It appears, however, that this assumption may affect only isotropic source radiation, since for perpendicular incidence the calculation shows good agreement with experimental results, as will be shown later on.

a — Detector Located Behind Two Parallel Barriers

The detector is assumed to be located behind two square barriers separated by a distance H . This geometry is shown in Figure A-1. The top barrier is covered by a uniform, plane monodirectional source of energy E_0 . The barrier closer to the detector (the bottom barrier) receives only those photons that emerge from the top

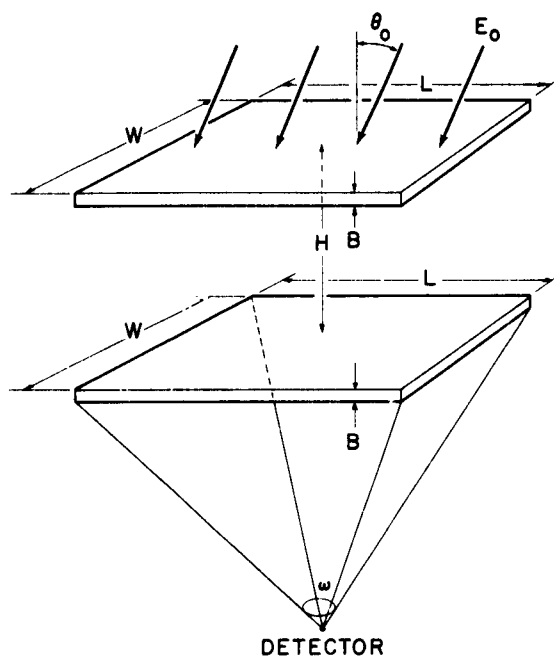


Figure A-1. Detector Located Behind Two Parallel Barriers

barrier with direction cosines such that they will strike the bottom barrier. (These photons may have been either unattenuated or scattered. However, as in Case I (p. 2) the detector responds only to the scattered radiation.) The histories of these photons are then followed in the bottom barrier to determine if they will be transmitted through the lower barrier within the solid angle subtended by the lower barrier at the detector.* In other words the only photons that are scored at the detector are those that are transmitted through the top barrier, hit the bottom barrier, and arrive at the detector (undergoing at least one collision between source and detector).

b — Detector Located Behind Three Parallel Barriers

This case, shown in Figure A-2, is similar to configuration a (Figure A-1) except that there is an additional barrier between source and detector. Photons arriving at the detector must first pass each barrier and must have the proper direction cosines to enter the following barrier. The photons emerging from the bottom

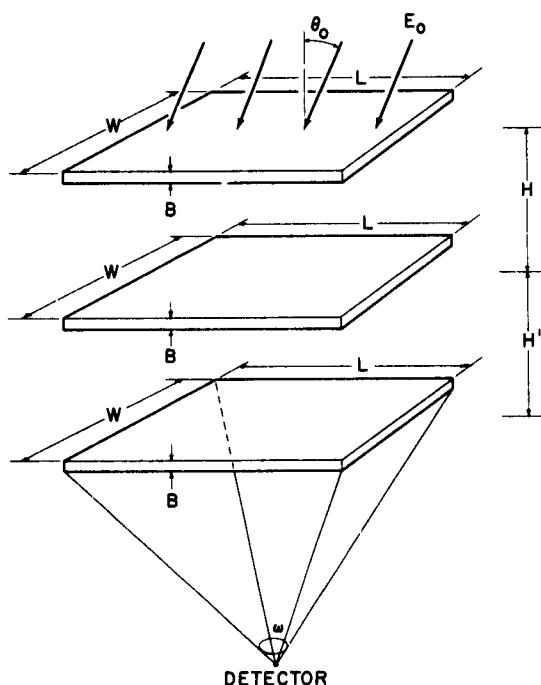


Figure A-2. Detector Located Behind Three Parallel Barriers

* Photons that enter the lower barrier and are subsequently backscattered do not contribute to the detector below the bottom barrier.

barrier must fall within the barrier-detector solid angle and must have energies less than the initial energy.

Table A-1 contains the data of scattered dose pertaining to configuration a. The thickness of each barrier corresponds to 20.5 psf. The results are given for three separation distances as a function of the solid angle fraction that the bottom barrier subtends at the detector. The separation distances are indicated by ratios of H/L , barrier-separation distance divided by the length of the barrier ($H/L = 1/4$, $1/2$, and 1). By way of comparison, the results for zero separation distance $H/L = 0$ (Table 2, p. 16) are also given. The effect produced by separating the barriers depends markedly on the angle of incidence, particularly for higher values of ω and H/L .

The results pertaining to configuration b are given in Table A-2. Three barriers, each of 20.5 psf, are separated by four combinations of H/L and H'/L , the upper separation distance divided by the length of the barrier and the lower separation distance divided by the length of the barrier. The combinations of the ratios are $1/2:1/2$, $1/2:1$, $1:1/2$, and $1:1$. The results for zero separation (Table 2, p. 19) are tabulated for comparison. As for the case of two separated barriers, the scattered dose depends upon the separation and angle of incidence.

Figure A-3 shows the scattered dose (in keV/g normalized to a source strength of 1 incident photon/cm²) from a 1.25 MeV plane isotropic source on the top of the first barrier. The results are given for the detector located behind the second slab as a function of solid angle fraction, ω , with respect to the bottom barrier for various separation distances (distance between detector and source) between slabs of 20.5 psf. Figure A-4 shows the scattered doses plotted against the solid angle fraction, ω , the top barrier subtends at the detector. Similar curves are shown for three barriers in Figures A-5 and A-6. The scattered dose for various slab separations versus the solid angle fraction, ω , with respect to the bottom slab is shown in Figure A-5, and Figure A-6 shows the scattered dose plotted against the solid angle fraction with respect to the top barrier.

Comparison of these calculations with experiments performed at Tech/Ops is shown in Figure A-7. The experiments were performed with an array of four vertical iron slabs each 2 ft x 2 ft, spaced 1 ft apart. The mass thickness of each slab was

20.5 psf. A parallel beam of 1.25 MeV gamma radiation was incident normal to the first slab. Three detectors were placed along the center line between the first two slabs at distance 2 in., 6 in., and 10 in. from the first slab. The points on the graph in Figure A-7a are the experimental results, and the dashed curve represents the results of Monte Carlo calculations for a detector between two slabs, as in the experiment, but with the third and fourth slabs absent (combination of Cases I and II, pp. 2,3). The solid curve represents the results of Monte Carlo calculations where only the first slab is present (Case I, p. 2). Figure A-7b shows the experimental results (points) for the situation where the detectors are placed 2 in., 6 in., and 10 in. behind the second slab. The solid curve gives the Monte Carlo results where only the first and second slabs are present (configuration a). Figure A-7c corresponds to the experiment where the three detectors are placed between the third and fourth slabs. The results (solid curve) of the Monte Carlo calculations, where there is no fourth slab, are shown (b).

The calculational results as displayed in form of curves in Figures A-3 to A-6 indicate a higher scattered dose behind separated barriers. This, however, ^{*} might very well be considered an overestimation of the actual (finite) barrier case, inherent in the design of the Monte Carlo approach chosen for this problem (uniform illumination of the bottom slab from radiation emanating from a finite portion of an infinite top barrier). As mentioned before, this peculiarity appears to affect only isotropically incident source radiation, since for perpendicular incidence the calculations show good agreement with experimental results (Figure A-7). To definitely determine the degree of validity of the approximation used in the calculation described in the appendix, a straight-forward Monte Carlo calculation for finite barriers would be necessary.

^{*}As was indicated earlier in this appendix.

TABLE A-1
DOSE DUE TO SCATTERING OF PHOTONS THROUGH
TWO IRON SLABS, EACH OF 20.5 psf MASS THICKNESS*†
(KeV/g normalized to 1 photon/cm²)

ω	H/L^\ddagger			
	0	1/4	1/2	1

$\cos \Theta_0 = 1.0$				
0.02	0.568	0.568	0.566	0.564
0.04	1.27	1.27	1.27	1.26
0.08	2.09	2.09	2.09	2.07
0.10	2.54	2.54	2.53	2.51
0.20	4.19	4.19	4.17	4.13
0.30	5.14	5.14	5.12	5.07
0.50	6.47	6.46	6.43	5.98
0.70	7.50	7.48	7.40	6.79
0.90	8.04	8.03	7.93	7.28
1.00	8.32	8.31	8.21	7.57

$\cos \Theta_0 = 0.75$				
0.02	0.288	0.288	0.287	0.280
0.04	0.504	0.504	0.503	0.493
0.08	1.01	1.01	0.997	0.975
0.10	1.23	1.23	1.22	1.18
0.20	2.55	2.54	2.52	2.42
0.30	3.75	3.74	3.71	3.56
0.50	5.96	5.94	5.87	5.09
0.70	7.55	7.52	7.25	6.17
0.90	8.64	8.60	8.30	7.14
1.00	8.92	8.87	8.57	7.41

* 5000 photons of energy 1.25 MeV are assumed incident on the first slab with angles for each of the five cases given by $\cos \Theta_0 = 1.0, 0.75, 0.50, 0.25$, and 0.0 .

† Results for isotropic incidence are obtained by integration of the monodirectional data.

‡ H/L gives slab separations (ratio of separation distance to length of slab).

TABLE A-1 (Cont'd.)
DOSE DUE TO SCATTERING OF PHOTONS THROUGH
TWO IRON SLABS, EACH OF 20.5 psf MASS THICKNESS
(KeV/g normalized to 1 photon/cm²)

ω	H/L			
	0	1/4	1/2	1

Cos Θ_0 = 0.50				
0.02	0.125	0.125	0.122	0.0624
0.04	0.287	0.287	0.279	0.157
0.08	0.608	0.603	0.589	0.354
0.10	0.744	0.738	0.722	0.431
0.20	1.70	1.70	1.65	0.903
0.30	2.62	2.60	2.53	1.31
0.50	5.02	4.99	4.85	1.68
0.70	7.25	7.19	6.80	1.86
0.90	8.87	8.70	8.02	1.91
1.00	9.21	9.05	8.34	1.92

Cos Θ_0 = 0.25				
0.02	0.0884	0.0835	0.070	0.0615
0.04	0.201	0.196	0.157	0.139
0.08	0.411	0.402	0.322	0.282
0.10	0.510	0.501	0.404	0.358
0.20	1.13	1.11	0.869	0.759
0.30	1.71	1.69	1.29	1.10
0.50	3.21	3.16	2.30	1.35
0.70	5.79	5.19	3.12	1.48
0.90	6.56	6.39	3.35	1.55
1.00	6.77	6.60	3.44	1.60

TABLE A-1 (Cont'd.)
DOSE DUE TO SCATTERING OF PHOTONS THROUGH
TWO IRON SLABS, EACH OF 20.5 psf MASS THICKNESS
(KeV/g normalized to 1 photon/cm²)

ω	H/L			
	0	1/4	1/2	1

Cos Θ_0 = 0.0				
0.02	0.0491	0.0491	0.0485	0.0407
0.04	0.0812	0.0812	0.0780	0.0668
0.08	0.180	0.180	0.173	0.154
0.10	0.232	0.232	0.223	0.201
0.20	0.420	0.420	0.402	0.331
0.30	0.714	0.711	0.666	0.559
0.50	1.35	1.33	1.21	0.706
0.70	1.88	1.85	1.56	0.792
0.90	2.15	2.09	1.72	0.876
1.00	2.18	2.13	1.76	0.913

Isotropic				
0.02	0.203	0.201	0.197	0.176
0.04	0.417	0.416	0.403	0.363
0.08	0.790	0.786	0.760	0.681
0.10	0.966	0.962	0.930	0.831
0.20	1.92	1.91	1.83	1.58
0.30	2.75	2.74	2.60	2.19
0.50	4.53	4.35	4.21	2.74
0.70	6.19	6.14	5.41	3.32
0.90	7.29	7.19	6.12	3.67
1.00	7.54	7.44	6.33	3.79

TABLE A-2

DOSE DUE TO THE SCATTERING OF PHOTONS THROUGH THREE
IRON SLABS, EACH OF 20.5 psf MASS THICKNESS*†
(KeV/g normalized to 1 photon/cm²)

ω	H/L: H'/L [†]				
	0:0	$\frac{1}{2}:\frac{1}{2}$	$\frac{1}{2}:1$	$1:\frac{1}{2}$	1:1

$\cos \Theta_0 = 1.00$

0.02	0.475	0.469	0.459	0.464	0.457
0.04	1.03	1.02	1.00	1.01	0.999
0.08	1.78	1.77	1.74	1.75	1.73
0.10	2.24	2.22	2.17	2.18	2.16
0.20	3.73	3.70	3.62	3.64	3.60
0.30	4.76	4.71	4.59	4.63	4.57
0.50	5.88	5.81	5.36	5.62	5.34
0.70	6.66	6.52	5.98	6.31	5.95
0.90	7.05	6.90	6.30	6.67	6.27
1.00	7.20	7.06	6.43	6.83	6.40

$\cos \Theta_0 = 0.75$

0.02	0.267	0.262	0.255	0.252	0.248
0.04	0.529	0.521	0.505	0.510	0.497
0.08	0.955	0.946	0.908	0.921	0.890
0.10	1.19	1.17	1.12	1.14	1.10
0.20	2.31	2.26	2.18	2.20	2.15
0.30	3.25	3.18	3.04	3.08	2.98
0.50	4.96	4.85	3.98	4.48	3.90
0.70	6.07	5.82	4.66	5.36	4.57
0.90	6.61	6.24	5.00	5.76	4.92
1.00	6.83	6.47	5.18	5.99	5.10

* 5000 photons of energy 1.25 MeV are assumed incident on the first slab with angles for each of the five cases given by $\cos \Theta_0 = 1.0, 0.75, 0.50, 0.25$, and 0.00 .

† Results for isotropic incidence are obtained by integration of the mono-directional data.

‡ H/L: H'/L gives upper and lower slab separations, respectively (ratio of separation distance to length of slab).

TABLE A-2 (Cont'd.)

DOSE DUE TO THE SCATTERING OF PHOTONS THROUGH THREE
IRON SLABS, EACH OF 20.5 psf MASS THICKNESS
(KeV/g normalized to 1 photon/cm²)

ω	H/L: H'/L				
	0:0	$\frac{1}{2}:\frac{1}{2}$	$\frac{1}{2}:1$	$1:\frac{1}{2}$	1:1
Cos $\Theta_o = 0.50$					
0.02	0.0995	0.0942	0.0887	0.0350	0.0350
0.04	0.188	0.173	0.152	0.0803	0.0803
0.08	0.423	0.402	0.319	0.182	0.180
0.10	0.507	0.476	0.375	0.209	0.207
0.20	1.13	1.06	0.807	0.442	0.438
0.30	1.17	1.68	1.27	0.679	0.671
0.50	3.07	2.92	1.59	0.854	0.818
0.70	4.28	3.84	1.78	0.995	0.936
0.90	4.92	4.32	1.87	1.06	0.982
1.00	5.13	4.52	1.96	1.15	1.07
Cos $\Theta_o = 0.25$					
0.02	0.0550	0.0402	0.0402	0.0344	0.0344
0.04	0.115	0.0839	0.0831	0.0757	0.0757
0.08	0.242	0.177	0.175	0.156	0.156
0.10	0.301	0.211	0.207	0.188	0.188
0.20	0.619	0.422	0.399	0.338	0.337
0.30	1.02	0.672	0.604	0.502	0.498
0.50	1.68	1.07	0.720	0.646	0.596
0.70	2.48	1.42	0.788	0.716	0.651
0.90	2.92	1.49	0.843	0.767	0.702
1.00	2.94	1.49	0.843	0.767	0.702

TABLE A-2 (Cont'd.)

DOSE DUE TO THE SCATTERING OF PHOTONS THROUGH THREE
IRON SLABS, EACH OF 20.5 psf MASS THICKNESS
(KeV/g normalized to 1 photon/cm²)

ω	H/L: H'/L				
	0:0	$\frac{1}{2}:\frac{1}{2}$	$\frac{1}{2}:1$	$1:\frac{1}{2}$	1:1

$\cos \theta_0 = 0.00$

0.02	0.0364	0.0346	0.0338	0.0310	0.0303
0.04	0.0516	0.0468	0.0426	0.0371	0.0358
0.08	0.106	0.0990	0.0932	0.0826	0.0813
0.10	0.147	0.140	0.134	0.122	0.121
0.20	0.228	0.216	0.192	0.171	0.168
0.30	0.344	0.322	0.287	0.256	0.250
0.50	0.615	0.548	0.372	0.347	0.316
0.70	0.796	0.650	0.414	0.383	0.352
0.90	0.858	0.696	0.437	0.406	0.371
1.00	0.906	0.721	0.441	0.411	0.375

Isotropic

0.02	0.169	0.162	0.162	0.142	0.140
0.04	0.343	0.328	0.316	0.297	0.293
0.08	0.641	0.615	0.580	0.543	0.533
0.10	0.796	0.760	0.714	0.672	0.659
0.20	1.51	1.43	1.32	1.22	1.20
0.30	2.15	2.01	1.84	1.68	1.64
0.50	3.24	3.01	2.29	2.24	2.03
0.70	4.14	3.67	2.61	2.60	2.33
0.90	4.60	3.96	2.77	2.78	2.48
1.00	4.74	4.09	2.86	2.88	2.56

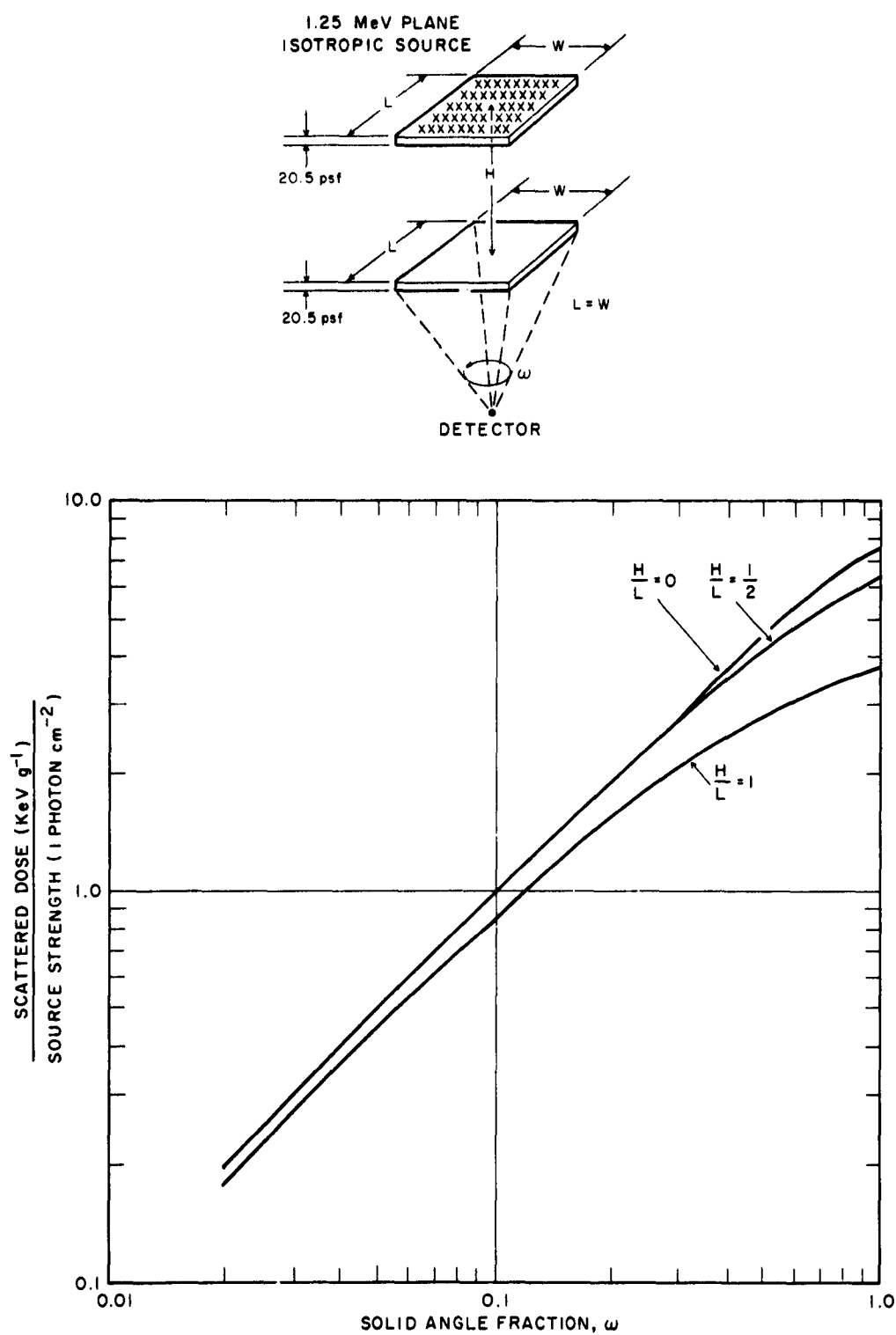


Figure A-3. Dose Due to Scattering of Photons Through Two Separated Iron Slabs, Each of Mass Thickness 20.5 psf ($H/L = 1/4, 1/2, 1$), and an Iron Slab of Mass Thickness 41.0 psf ($H/L = 0$) vs Solid Angle Fraction

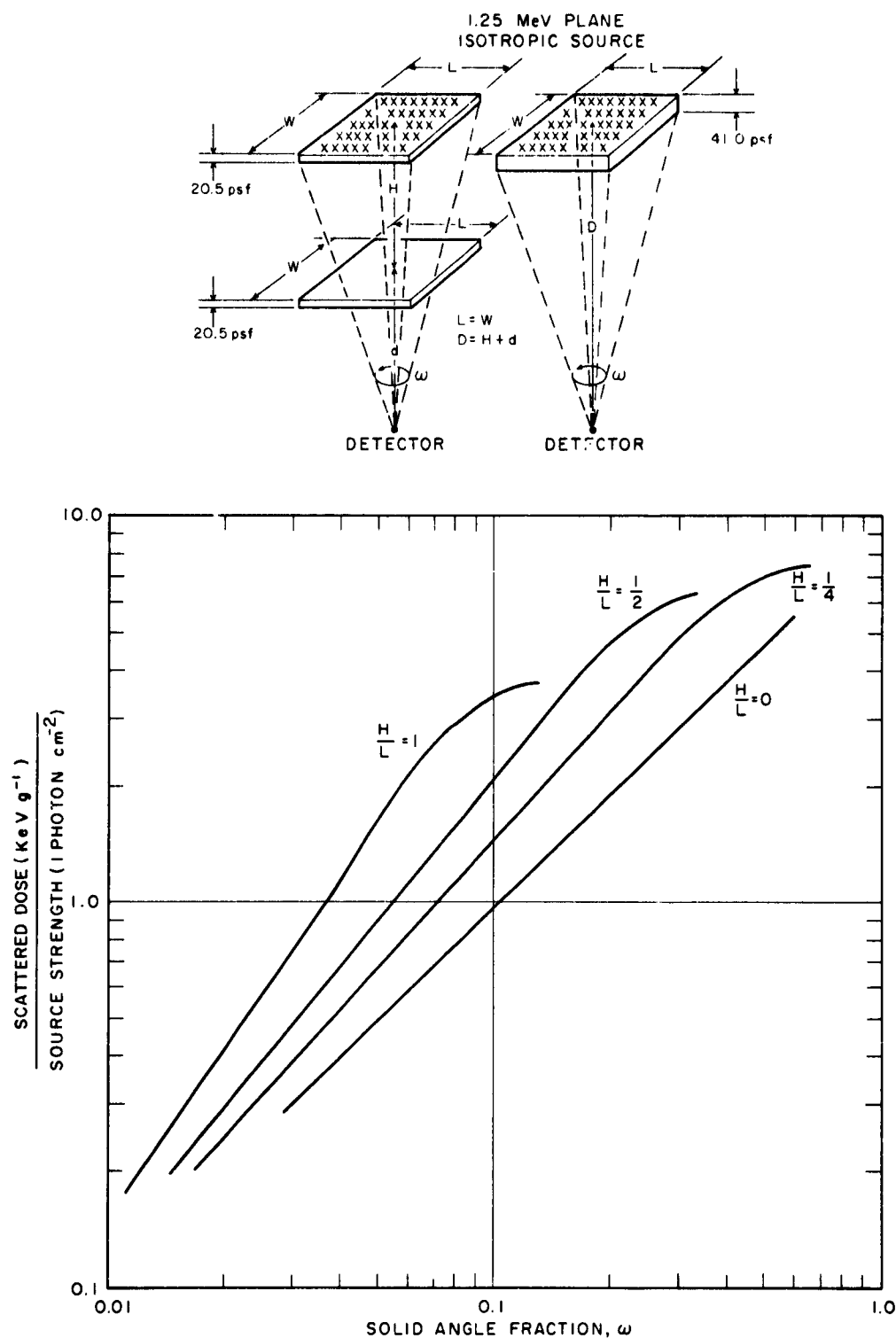


Figure A-4. Dose Due to Scattering of Photons Through Two Separated Iron Slabs, Each of Mass Thickness 20.5 psf ($H/L = 1/4, 1/2, 1$), and an Iron Slab of Mass Thickness 41.0 psf ($H/L = 0$) vs Solid Angle Fraction Subtended by the Top Barrier

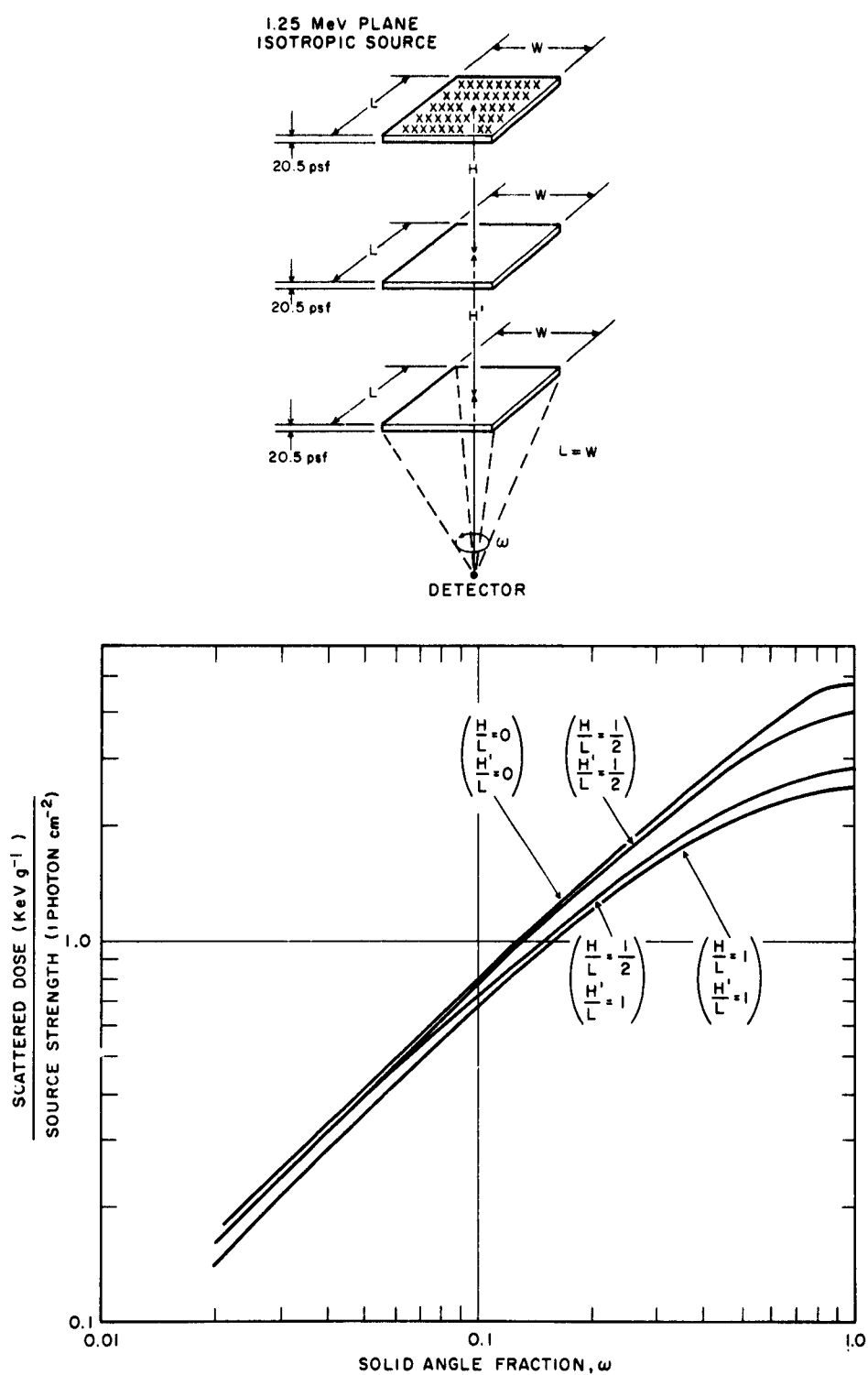


Figure A-5. Dose Due to Scattering of Photons Through Three Separated Iron Slabs of Mass Thickness 20.5 psf ($H/L:H'/L = 1/2:1/2, 1/2:1, 1:1/2, 1:1$) and an Iron Slab of Mass Thickness 61.5 psf ($H/L = H'/L = 0$) vs Solid Angle Fraction

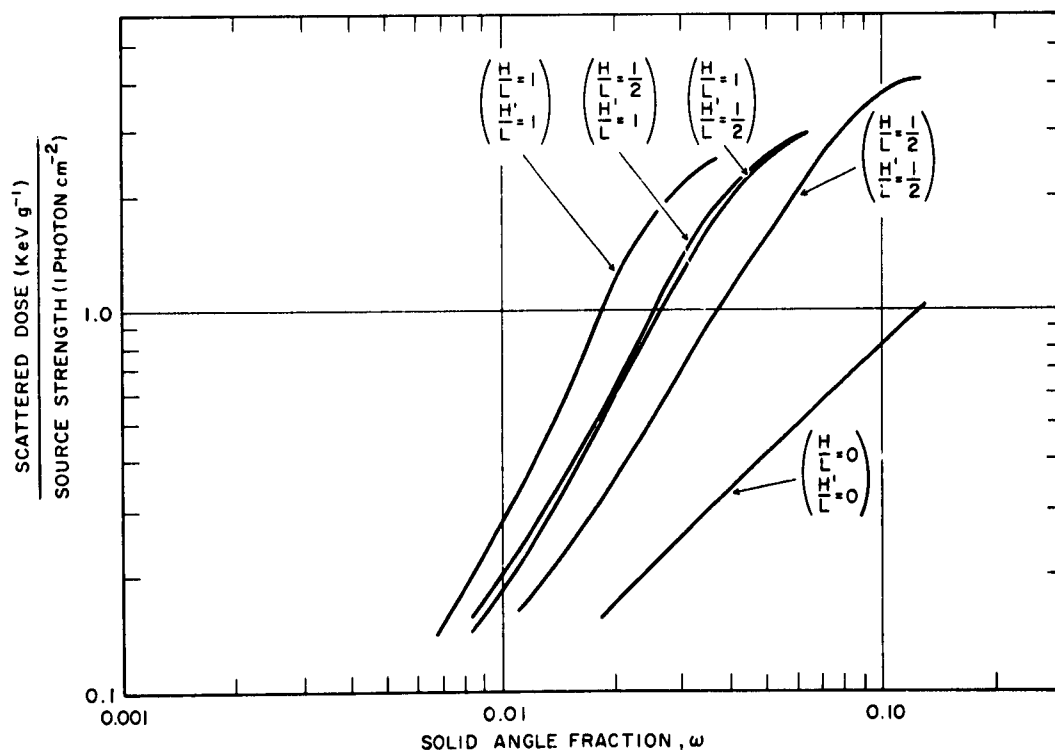
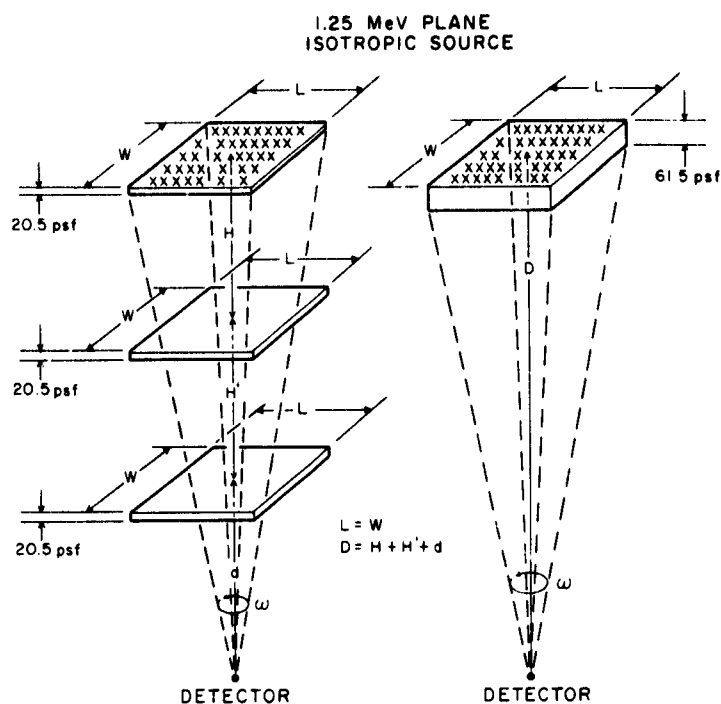


Figure A-6. Dose Due to Scattering of Photons Through Three Separated Iron Slabs of Mass Thickness 20.5 psf ($H/L:H'/L = 1/2:1/2, 1/2:1, 1:1/2, 1:1$) and an Iron Slab of Mass Thickness 61.5 psf ($H/L = H'/L = 0$) vs Solid Angle Fraction Subtended by the Top Barrier

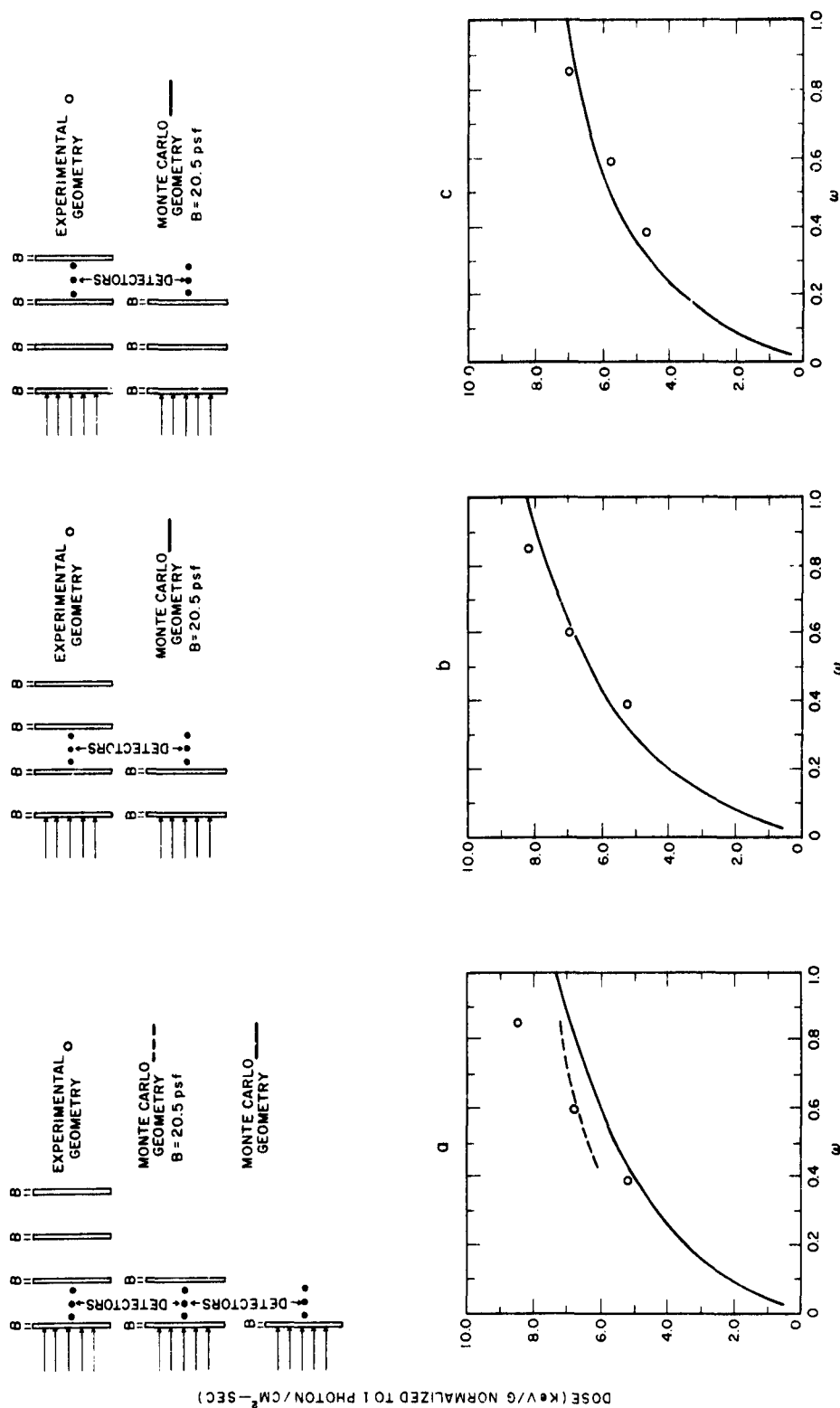


Figure A-7. Comparison of Dose Calculated by the Monte Carlo Method with that Obtained Experimentally for Normally Incident Co-60 Radiation

<p>Rpt No. 64-49 Raso, D. J., and Woolf, Stanley THE DOSE RESULTING FROM 1.25 MeV PLANE SOURCE BEHIND VARIOUS ARRANGEMENTS OF IRON BARRIERS. Technical Operations, Inc., Burlington, Mass. Office of Civil Defense, De- partment of Defense, Washington, D. C. Final Report, June, 1964. 47 p., incl. 13 figs., 9 tables.</p> <p>Unclassified Report</p> <p>Calculations were performed by the Monte Carlo method to determine the dose at various positions behind parallel barriers (circular or rectangular). In some cases, the parallel barriers were sepa- rated. Also, calculations were made for a block- house geometry. The results were obtained for a 1.25 MeV plane monodirectional source (angles of</p> <p>(over)</p>	<p>1. The Dose Resulting from 1.25 MeV Plane Source Behind Various Arrangements of Iron Barriers</p> <p>2. Gamma Ray Dose</p> <p>3. Separated Barrier</p> <p>4. Blockhouse</p> <p>5. Raso, D. J. Woolf, S.</p> <p>6. Office of Civil Defense</p> <p>7. Contract OCD-OS- 62-219</p> <p>(over)</p>	<p>Rpt No. 64-49 Raso, D. J., and Woolf, Stanley THE DOSE RESULTING FROM 1.25 MeV PLANE SOURCE BEHIND VARIOUS ARRANGEMENTS OF IRON BARRIERS. Technical Operations, Inc., Burlington, Mass. Office of Civil Defense, De- partment of Defense, Washington, D. C. Final Report, June, 1964. 47 p., incl. 13 figs., 9 tables.</p> <p>Unclassified Report</p> <p>Calculations were performed by the Monte Carlo method to determine the dose at various positions behind parallel barriers (circular or rectangular). In some cases, the parallel barriers were sepa- rated. Also, calculations were made for a block- house geometry. The results were obtained for a 1.25 MeV plane monodirectional source (angles of</p> <p>(over)</p>	<p>1. The Dose Resulting from 1.25 MeV Plane Source Behind Various Arrangements of Iron Barriers</p> <p>2. Gamma Ray Dose</p> <p>3. Separated Barrier</p> <p>4. Blockhouse</p> <p>5. Raso, D. J. Woolf, S.</p> <p>6. Office of Civil Defense</p> <p>7. Contract OCD-OS- 62-219</p> <p>(over)</p>	<p>incidence given by $\cos \theta_0 = 0.0, 0.25, 0.50, 0.75, 1.0$, and isotropic) incident on 20.5, 41.0, and 61.5 psf of iron. Comparisons were made with roof reduction factors obtained by Spencer and with experiments performed at Technical Opera- tions Research.</p>
--	--	--	--	--